AD-A188 984 NEUTRAL BEAM PROPAGATION THROUGH THE ATMOSPHERE(U) 1/1
BOSTON COLL CHESTNUT HILL MA DEPT OF PHYSICS
G J KALMAN ET AL. 15 JUN 87 AFGL-TR-87-0267
UNCLASSIFIED F19628-84-K-0039 F/G 19/12 NL

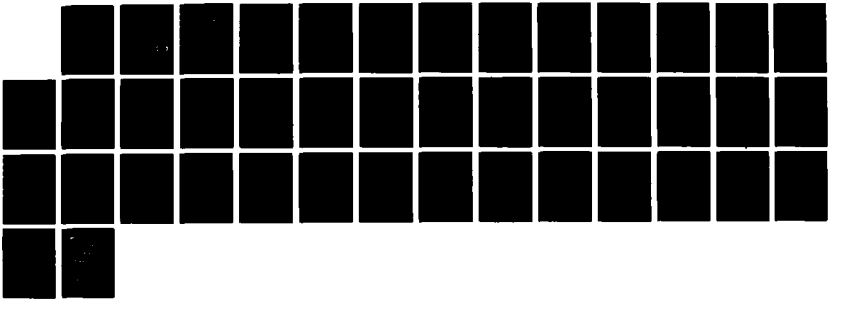

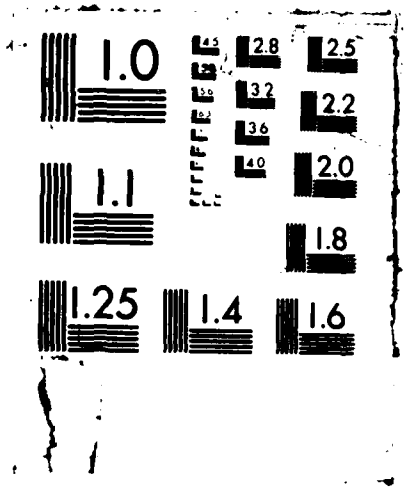
1.0
1.1
1.25
1.4
1.6
1.8
2.0
2.2
2.5
2.8
3.2
3.6
4.0

(4)

AFGL-TR-87-0267

AD-A188 984

DTIC FILE COPY

Neutral Beam Propagation Through the Atmosphere

Gabor J. Kalman
T. Li

Boston College
Department of Physics
Chestnut Hill, MA 02167

15 June 1987

Final Report
1 June 1984 - 1 June 1987

APPROVED FOR PUBLIC RELEASE; DISTRIBUTION UNLIMITED

AIR FORCE GEOPHYSICS LABORATORY
AIR FORCE SYSTEMS COMMAND
UNITED STATES AIR FORCE
HANSCOM AIR FORCE BASE, MASSACHUSETTS 01731

"This technical report has been reviewed and is approved for publication"

SHU T. LAI
Contract Manager

WILLIAM J. BURKE
Branch Chief

FOR THE COMMANDER

RITA C. SAGALYN,
Division Director

This report has been reviewed by the ESD Public Affairs Office (PA) and is releasable to the National Technical Information Service (NTIS).

Qualified requestors may obtain additional copies from the Defense Technical Information Center. All others should apply to the National Technical Information Service.

If your address has changed, or if you wish to be removed from the mailing list, or if the addressee is no longer employed by your organization, please notify AFGL/DAA, Hanscom AFB, MA 01731. This will assist us in maintaining a current mailing list.

Do not return copies of this report unless contractual obligations or notices on a specific document requires that it be returned.

SECURITY CLASSIFICATION OF THIS PAGE AD-A188984

REPORT DOCUMENTATION PAGE

1a. REPORT SECURITY CLASSIFICATION Unclassified	1b. RESTRICTIVE MARKINGS
2a. SECURITY CLASSIFICATION AUTHORITY	3. DISTRIBUTION/AVAILABILITY OF REPORT Approved for public release; Distribution unlimited.
2b. DECLASSIFICATION/DOWNGRADING SCHEDULE	
4. PERFORMING ORGANIZATION REPORT NUMBER(S)	5. MONITORING ORGANIZATION REPORT NUMBER(S) AFGL-TR-87-0267
6a. NAME OF PERFORMING ORGANIZATION Boston College Department of Physics 6b. OFFICE SYMBOL (If applicable)	7a. NAME OF MONITORING ORGANIZATION Air Force Geophysics Laboratory
6c. ADDRESS (City, State, and ZIP Code) Chestnut Hill, MA 02167	7b. ADDRESS (City, State, and ZIP Code) Hanscom AFB Massachusetts 01731
8a. NAME OF FUNDING/SPONSORING ORGANIZATION 8b. OFFICE SYMBOL (If applicable)	9. PROCUREMENT INSTRUMENT IDENTIFICATION NUMBER F19628-84-K-0039
8c. ADDRESS (City, State, and ZIP Code)	10. SOURCE OF FUNDING NUMBERS PROGRAM ELEMENT NO. 62101F; PROJECT NO. 7661; TASK NO. 14; WORK UNIT ACCESSION NO AF

11 TITLE (Include Security Classification)

Neutral Beam Propagation through the Atmosphere

12 PERSONAL AUTHOR(S) Gabor J. Kalman, T. Li

13a. TYPE OF REPORT	13b. TIME COVERED	14. DATE OF REPORT (Year, Month, Day)	15 PAGE COUNT
Final	FROM June 1, 84 TO June 1, 87	1987 June 15	42

16 SUPPLEMENTARY NOTATION

17 COSATI CODES			18. SUBJECT TERMS (Continue on reverse if necessary and identify by block number)
FIELD	GROUP	SUB-GROUP	Neutral beam, Beam induced stripping, Stripping, Polarization, Ionization, Cross section

19 ABSTRACT (Continue on reverse if necessary and identify by block number)

The problem of Beam Induced Stripping (BIS) process, occuring when a neutral beam propagates through the Earth's atmosphere, has been analyzed. At high current densities the process is importnat and leads to a rapid disintegration of the beam. At lower current densities currently contemplated for experiments, the effect is probably not significant.

20 DISTRIBUTION/AVAILABILITY OF ABSTRACT ☐ UNCLASSIFIED/UNLIMITED ☐ SAME AS RPT. ☐ DTIC USERS	21. ABSTRACT SECURITY CLASSIFICATION Unclassified
22a NAME OF RESPONSIBLE INDIVIDUAL Shu T. Lai	22b TELEPHONE (Include Area Code) 22c. OFFICE SYMBOL AFGL/PHK

DD FORM 1473, 84 MAR 83 APR edition may be used until exhausted. All other editions are obsolete.

SECURITY CLASSIFICATION OF THIS PAGE

TABLE OF CONTENTS

LEGEND FOR FIGURES OUTSIDE THE TEXT

Fig. 3

T_f versus θ: T_f in unit of 1.138952×10^{-7} sec, θ in degree and n for beam energy in unit of MeV.

(a) n=1
(b) n=2
(c) n=5
(d) n=8
(e) n=10
(f) n=20
(g) n=30
(h) n=40
(i) n=50
(j) n=60
(k) n=70

Fig. 5

T_ϵ versus θ: T_ϵ in sec, θ in radian, and n for beam energy in unit of MeV.

(a) n=0.1
(b) n=1
(c) n=2
(d) n=10
(e) n=20
(f) n=40
(g) n=50
(h) n=70

Fig. 6

T_o versus θ: T_o from Eq.(15) with f=0 or δ=1; T_o in unit of 1.138952×10^{-7} sec, and θ in degree.

Fig. 7

$F(\psi)$ versus ψ: ψ in radian.

(a) ψ from 0 to 100 radians.
(b) ψ from 0 to 10 radians.

REFERENCE

T. Li, G. Kalman and P. Pulsifer: "Neutral Beam Propagation Through the Upper Atmosphere II" AFGL-TR-86-0192 (Report II) ADA182601

I. INTRODUCTION

Our previous work, hereafter referred to as Report II, concerned the beam attenuation due to "self-stripping" resulting from an "optimum" electric field having the components due to transverse and longitudinal polarization,

$$E_y = v_b B \sin\theta \tag{1}$$

$$E_z = v_b B \cos^2\theta \sin\theta \tag{2}$$

$$E_x = -v_b B \cos\theta \sin^2\theta \tag{3}$$

where v_b is the beam velocity, and $B = \sqrt{B_x^2+B_z^2}$, $B_z = B \sin\theta$, $B_x = B \cos\theta$ (See Figure 1).

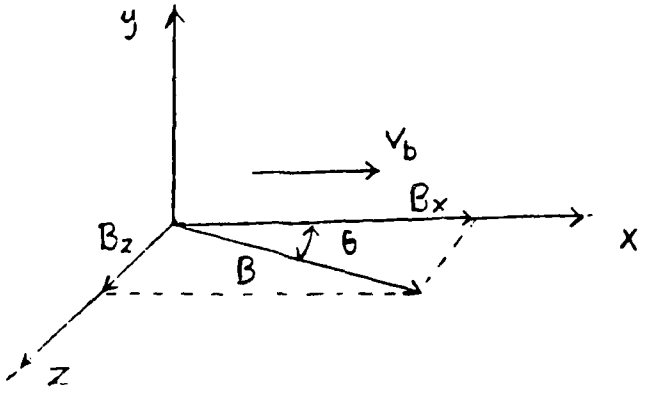

Figure 1

We assumed a confinement time $T_{\parallel}$ of the form

$$T_{\parallel} = \frac{2R_o}{v_b \sin^2\theta} \tag{4}$$

with $\theta < 90°$, and R_o being the beam radius.

We also assumed another confinement time τ given by

$$\cos(\omega\tau) = 1 - \frac{R_o}{R}, \text{ for } \theta < 90° \tag{5}$$

where $\omega = \frac{eB}{m_e}$ and R are respectively the electron gyrofrequency and gyroradius.

In the present work, we will study <u>alternative</u> models for the electric field, and the corresponding confinement times. Our purpose is twofold. First, we wish to study the effect of different reasonable models on the confinement time. Second, we wish to combine the confinement time (T) with the (energy dependent) collision cross section (σ) to obtain an estimate for

the total beam-induced stripping probability $P = \frac{T}{\sigma nv} = \frac{T}{\sigma J}$ as a function of the beam parameters.

II. ELECTRIC FIELD WITH TRANSVERSE COMPONENT ONLY: CONFINEMENT TIME

In the first model, the electric field has only one component, due to transverse polarization. More specifically, we have

$$E_y = f v_b B \sin\theta, \quad 0 \le f \le 1$$

$$E_z = 0$$

$$E_x = 0 \tag{6}$$

where f can be regarded as field strength parameter. $f = 1$ corresponds to a fully developed polarization field, while $f<1$ describes reduction due either to ambient plasma screening or to transient situations where the electric field has not fully developed.

The resulting electron velocity equation becomes

$$\dot{x}(t) = (1-f)\, v_b \sin^2\theta \cdot \cos(\omega t) + v_b\, (f \sin\theta \cdot \cos\theta) \tag{7}$$

$$\dot{y}(t) = (1-f)\, v_b \sin\theta \cdot \sin(\omega t) \tag{8}$$

$$\dot{z}(t) = (1-f)\, v_b \sin\theta \cdot \cos\theta \, [1-\cos(\omega t)] \tag{9}$$

For the field-free case, $f = 0$, we have

$$\dot{x}_o(t) = v_b \sin^2\theta \cdot \cos(\omega t) + v_b \cos^2\theta \tag{10}$$

$$\dot{y}_o(t) = v_b \sin\theta \cdot \sin(\omega t) \tag{11}$$

$$\dot{z}_o(t) = v_b \sin\theta \cdot \cos\theta \, [1-\cos(\omega t)] \tag{12}$$

For the "maximum" strength field: $f = 1$, we have $\dot{x}(t) = v_b$, $\dot{y}(t) = 0$, and $\dot{z}(t) = 0$ which describes undisturbed electron motion.

Integrations of Eqs. (8) and (9) give the trajectory equations

$$y(t) = (1-f)\, R \sin\theta \,[1-\cos(\omega t)] \tag{13}$$

$$z(t) = (1-f)\, R \sin\theta\cdot\cos\theta \,[\omega t - \sin(\omega t)], \tag{14}$$

where again ω and R are respectively the electron gyrofrequency and gyroradius.

The y(t) is sinusoidal and confined between 0 and $2(1-f)\, R \sin\theta$, while z(t) has a secular behavior due to drift.

The confinement time can be considered in the following manner. Looking along the positive x-axis, we can interpret the interception of y-z trajectory with the beam (radius R_o) circumference as equivalent to confinement time T_f (See Figure 2)

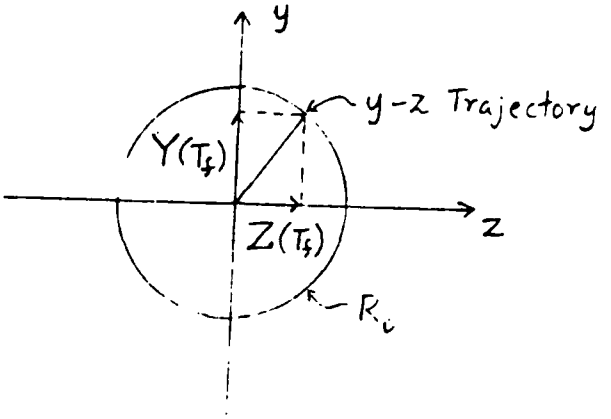

Figure 2

We can now write

$$Y^2(T_f) + Z^2(T_f) = R_o^2$$

or more specifically

$$\sin^2\theta\,[1-\cos(\omega T_f)]^2 + \sin^2\theta\cdot\cos^2\theta[\omega\tau - \sin(\omega T_f)]^2 = \frac{\gamma^2}{(1-f)^2}\,, \tag{15}$$

where $\gamma = R_o/R$. Computer-generated results from Eq. (15) in the form of $T_f = T_f(\theta,\gamma)$ are given in Figs. 3(a) to 3(n). Assuming R_o to have a fixed value of 10cm, we have $\gamma = \frac{6.34517\times10^{-2}}{n}$, with n being the beam energy E_b in unit of MeV.

It is worth noting that T_o represents the confinement time for the zero-field case, while T_1 represents the confinement time for "optimum" y-component-only field; T_f is infinite, since the optimum y-component-only field results in undisturbed electron drift.

However, T_f can be considered in another way. From Eqs. (13) and (14), we write

$$Y = (1-f)\, R \sin\theta\, (1-\cos \omega T_f) = \frac{1}{A}\,(1-\cos\omega T_f),$$

$$Z = (1-f)\, R \sin\theta\cdot\cos\theta\, (\omega T_f - \sin\omega T_f) = \frac{1}{B}\,(\omega T_f - \sin\omega T_f),$$

where $\frac{1}{A} = (1-f)\, R \sin\theta$ and $\frac{1}{B} = (1-f)\, R \sin\theta\cdot\cos\theta$. Rearranging terms and squaring, we obtain a quadratic equation for T_f,

$$\omega^2 T_f^2 - 2\omega BZ T_f + T_f + B^2Z^2 - 2AY = 0,$$

which yields the solution

$$T_f = \frac{B}{\omega} \pm [2AY - A^2Y^2]^{1/2} \tag{16}$$

It is instructive to compare Eq. (16) with Eq. (4). If we let $Y \equiv 0$, we get

$$T_f(Y=0) = \frac{BZ}{\omega} = \frac{BR_o}{\omega} = \frac{2R_o}{(1-f)v_b\sin^2\theta} = \frac{T_\parallel}{(1-f)}, \tag{17}$$

where we have made use of the relation,

$$Z^2 + Y^2 = R_o^2, \text{ i.e., } Z = R_o \text{ for } Y \equiv 0.$$

For the zero-field case($f = 0$) we obtain

$$T_\parallel = T_o(Y=0)$$

Thus, we have clarified the approximation involved in the confinement time $T_\parallel$ as used in Report II. In other words, $T_\parallel$ is equal to the zero-field confinement time with the approximation of having $Y = 0$. In the following we will examine closely various types of confinement times and their comparative

merits.

III. ELECTRIC FIELD WITH "OPTIMUM" STRENGTH: CONFINEMENT TIME

The "optimum" electric field as given by Eqs. (1), (2) and (3) results in the following y-z trajectory equations:

$$y_\varepsilon(t) = R\sin\theta\cdot\cos\theta\ [\omega t-\sin(\omega t)] \tag{19}$$

$$z_\varepsilon(t) = -R\sin\theta\cdot\cos^2\theta\ [1-\cos(\omega t)] \tag{20}$$

where the subscript ε denotes "optimum" field strength.

Recalling the corresponding field-free equations as given in Eqs. (11) and (12), we can write

$$y_\varepsilon(t) = z_o(t), \tag{21}$$

$$z_\varepsilon(t) = -\cos^2\theta.\ y_o(t) \tag{22}$$

which can be graphically described in Fig. 4.

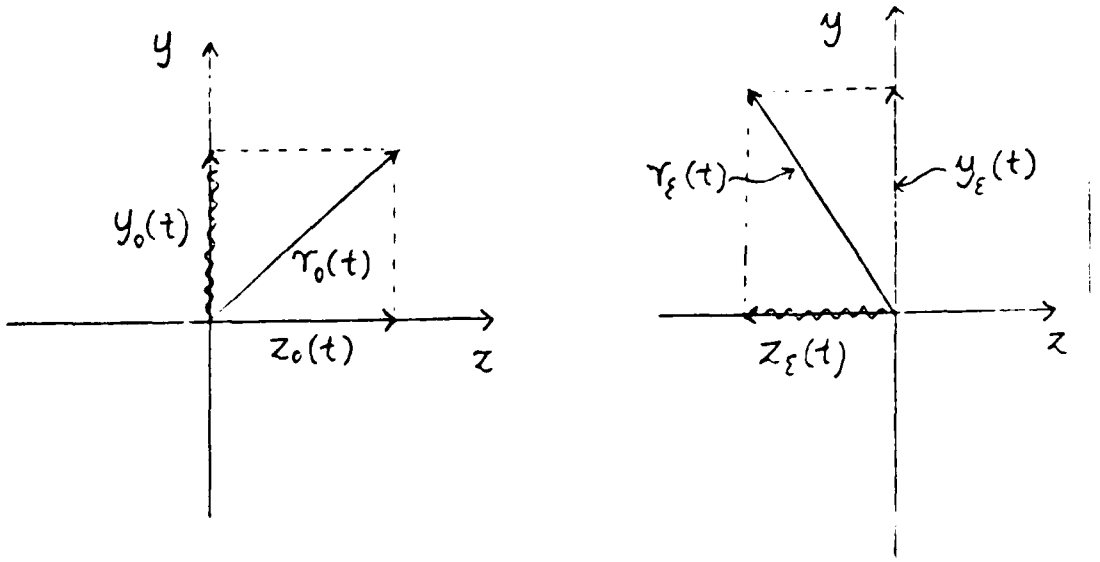

Figure 4

The switching-on of optimum field has the effect of rotating the y-z trajectory about the x-axis through 90° and reducing z projection by a factor of $\cos^2\theta$. Specifically, we have

$$r_o^2(t) = y_o^2(t) + z_o^2(t) \tag{23}$$

$$r_\varepsilon^2(t) = y_\varepsilon^2(t) + z_\varepsilon^2(t)$$

$$= \cos^4\theta\ y_o^2(t) + z_o^2(t) \tag{24}$$

which shows that $r_\varepsilon(t)$ is less than $r_o(t)$ except at $\theta = 0°$. Consequently, the confinement time T_ε from $r_\varepsilon(T_\varepsilon)=R$ is longer than the field-free value T_o from $r_o(T_o)=R_o$.

To obtain T_ε, we set

$$\gamma_\varepsilon^2(T_\varepsilon) = y_\varepsilon^2(T_\varepsilon) + z_\varepsilon^2(T_\varepsilon) = R_o^2 \tag{25}$$

which can be re-expressed as

$$\frac{\gamma^2}{\sin^2\theta\ \mathrm{coz}^2\theta} = \omega^2 T_\varepsilon^2 - 2\omega T_\varepsilon \cdot \sin\omega T_\varepsilon \cdot - 2\cos\theta \cdot \cos\omega T_\varepsilon$$

$$+ 2\cos^2\theta + \sin^2\theta \cdot \sin^2\omega T_\varepsilon \tag{26}$$

where the dimensionless parameter $\gamma = \frac{R_o}{R} = 6.34517 \times 10^{-2}/\sqrt{n}$, with $R_o = 10\mathrm{cm}$ and n is beam energy in unit of Mev.

Computer-generated results for T_ε are shown in Figs. 5(a) through 5(h). It is worth noting that at $\theta = 45°$, T_ε is about 1.2×10^{-7} sec for beam energies ranging from 1 to 70 Mev.

IV. ELECTRIC FIELD WITH FRACTIONAL STRENGTH: IMPACT ENERGY.

A field of less-than-optimum strength can be expressed as

$$Ey = f\ v_b\ B\ \sin\theta \tag{27}$$

$$E_z = g v_b\ B\ \sin\theta \cdot \cos^2\theta \tag{28}$$

$$E_x = -gv_b B \sin^2\theta\cdot\cos\theta \tag{29}$$

where both f and g are respectively $0<f<1$ and $0<g<1$. f and g can be interpreted as before in Section II, as representing ambient plasma screening and transient effects.

The resulting (electron) velocity equations are

$$\dot{x}(t) = -\delta v_b \sin^2\theta\cdot[1-\cos(\omega t)] + gv_b \sin^2\theta\cdot\cos\theta\cdot\sin(\omega t) + v_b \tag{30}$$

$$\dot{y}(t) = \delta v_b \sin\theta\cdot\sin(\omega t) + gv_b \sin\theta\cdot\cos\theta\ [1-\cos(\omega t)] \tag{31}$$

$$\dot{z}(t) = \delta v_b \sin\theta\cdot\cos\theta\ [1-\cos(\omega t)] - gv_b \sin\theta\cdot\cos^2\theta\cdot\sin(\omega t) \tag{32}$$

where we have written $\delta = 1-f$.

Integration of Eqs. (31) and (32) gives

$$y(t) = \delta R \sin\theta\cdot[1-\cos(\omega t)] + gR \sin\theta\cdot\cos\theta\cdot[\omega t-\sin(\omega t)] \tag{33}$$

$$z(t) = \delta R \sin\theta\cdot\cos\theta\cdot[\omega t-\sin(\omega t)] - gR \sin\theta\cdot\cos^2\theta[1-\cos(\omega t)] \tag{34}$$

where we have again written $\frac{v_b}{\omega} = R$, the electron gyroradius.

Now both y and z have secular drift components. The relative electron-beam velocity components are

$$v_x = -\delta v_b \sin^2\theta\,[1-\cos(\omega t)] + gv_b \sin^2\theta\cdot\cos\theta\cdot\sin(\omega t) \tag{35}$$

$$v_y = \delta v_b \sin\theta\cdot\sin(\omega t) + gv_b \sin\theta\cdot\cos\theta\cdot[1-\cos(\omega t)] \tag{36}$$

$$v_z = \delta v_b \sin\theta.\cos\theta\cdot[1-\cos(\omega t)] - gv_b \sin\theta\cdot\cos^2\theta\cdot\sin(\omega t) \tag{37}$$

Taking the time-average of the above quantities over the confinement time T, we have the time-averaged relative electron-beam velocity components:

$$\langle v_x\rangle = -\delta v_b \sin^2\theta.\left[1 - \frac{1}{\omega T}\sin(\omega T)\right] + gv_b \sin^2\theta\ \frac{1}{\omega T}\ [1-\cos(\omega T)] \tag{38}$$

$$\langle v_y\rangle = \delta v_b \sin^2\theta\cdot\frac{1}{\omega T}\ [1-\cos(\omega T)] + gv_b \sin\theta\cdot\cos\theta\cdot\left[1 - \frac{1}{\omega T}\sin(\omega T)\right] \tag{39}$$

$$\langle v_z \rangle = \delta v_b \sin\theta \cdot \cos\theta \cdot \left[1 - \frac{1}{\omega T}\sin(\omega T)\right] - g v_b \sin\theta \cdot \cos^2\theta \cdot \frac{1}{\omega T}\left[1-\cos(\omega T)\right] \tag{40}$$

As in our preceeding work, Report II, we define the electron-beam "impact energy" E_I as

$$E_I = \frac{1}{2}m\langle v\rangle^2 = \frac{1}{2}m\left[\langle v_x\rangle^2 + \langle v_y\rangle^2 + \langle v_z\rangle^2\right] \tag{41}$$

From Eqs. (38), (39) and (40), we obtain

$$E_I = E_b\left[(1-f)^2\sin^2\theta + g^2\sin^2\theta\cdot\cos^2\theta\right]F(T) \tag{42}$$

where $E_b = \frac{1}{2}mv_b^2$ is the beam energy, $1-f = \delta$ and

$$F(T) = 2\left(\frac{1}{\omega T}\right)^2\left[1-\cos(\omega T)\right] - 2\left(\frac{1}{\omega T}\right)\sin(\omega T) + 1 \tag{43}$$

More specifically, we rewrite Eq. (42) for three types of electric field models, namely, zero-field, y-component-only field and optimum field.

(i) Zero-Field:

We have $f = 0$ and $g = 0$

$$E_{IO} = E_b \sin^2\theta\ F(T_o) \tag{44}$$

(ii) Optimum Field:

We have $f = 1$ and $g = 1$

$$E_{I\epsilon} = E_b \sin^2\theta\cdot\cos^2\theta\cdot F(T_\epsilon) \tag{45}$$

(iii) Y-Component-Only Field:

We have $g = 0$,

$$E_{Iy} = E_b(1-f)^2\cdot\sin^2\theta\cdot F(T_f) \tag{46}$$

These three equations represent the field models with their corresponding confinement times, and will be considered in detail in the following section.

V. COMPARISON OF FIELD MODELS AND CONFINEMENT TIMES

In Report II, the zero-field model is represented by Eq. (40) of Report II, i.e.,

$$\frac{\langle v_{eb}\rangle_o^2}{v_b^2} = \sin^2\theta\{2(\frac{1}{\psi_e})^2[1-\cos(\psi_e)] + 1-2(\frac{1}{\psi_e})\sin(\psi_e)\}$$

which can be rewritten as

$$E_{IO} = E_b\sin^2\theta\cdot F(T_\parallel)$$

where $E_{IO} = \frac{1}{2}m_e\langle v_{eb}\rangle_o^2$, $E_b = \frac{1}{2}m_e v_b^2$, and $\psi_e = \omega T_\parallel$. We have now used the correct confinement T_o (as given by Fig. 6) instead of the approximate confinement time $T_\parallel = \frac{2R_o}{v_b\sin^2\theta}$.

Let us now compare the two confinement times $T_\parallel$ and T_o. As pointed out in Report II, $T_\parallel$ is symmetric with respect to $\theta = 45°$, but is <u>not</u> valid for $\theta \simeq 90°$. Both $T_\parallel$ and T_o are infinite as $\theta = 0°$ as they should, however, T_o approaches asymptotically its lowest value at $\theta = 90°$. Note that T_o is obtained from Eq. (15) with $f = 0$, and <u>re-entry</u> of electron into the beam is not considered. Therefore, at $\theta \simeq 90°$ and especially for $R \leq R_o$, T_o is, like $T_\parallel$, not valid.

For numerical comparison, let $R_o = 10$cm, $E_b = 1$ MeV and $\theta = 45°$; we then get $T_o = 4.45\times10^{-8}$s and $T_\parallel = 1.44\times10^{-8}$s. Note that $T_o > T_\parallel$ for $\theta < 80°$.

The result for the optimum field model in Report II was given by Eq. (44) of Report II, which is rewitten in the form

$$E_{I\varepsilon} = E_b\sin^2\theta\cdot\cos^2\theta\ F(T_\parallel).$$

Again, in our present result, as given by Eq.(44),

$$E_{I\varepsilon} = E_b \sin^2\theta \cdot \cos^2\theta \; F(T_\varepsilon),$$

we have used the correct confinement time T_ε instead of the approximate $T_\parallel$.

Figs. 5(a) through 5(h) show that T_ε is almost constant with a value of about 1.25×10^{-7}s for θ ranging from 45° to 75° and beam energy ranging from 1 MeV to 70 MeV. T_ε increases rapidly as θ approaches 0° and 90°. For numerical comparison, we let R_o = 10cm, E_b = 1 MeV and θ = 45°; we then get $T_\varepsilon = 1.25 \times 10^{-7}$s, thus we have $T_\varepsilon > T_o > T_\parallel$.

Now we come to the interesting and importand result as represented by Eq. (45),

$$E_{Iy} = E_b \left[(1-f)^2 \sin^2\theta \right] F(T_f).$$

Note that the "strength" parameter f plays an important role in determining the value of E_{Iy}. Especially for $f > 0.9$, T_f increases drastically and, as expected, is infinite at $f = 1$. [See Figs. 3(a) through 3(n)].

Again for numerical comparison, we let R_o = 10cm, E_b = 1 MeV and θ = 45°; we then get $T_{f=0.9} = 1.6 \times 10^{-7}$s, thus we have $T_{f=0.9} > T_\varepsilon > T_o > T_\parallel$.

Comparing the impact energies as given by Eqs.(44), (45) and (46), we have, for R_o = 10cm, E_b = 1 MeV and θ = 45°

$$E_{Io} = E_b \sin^2\theta \cdot F(T_o) = (1 \text{ MeV})\left(\frac{1}{\sqrt{2}}\right)^2 (0.2) = 100 \text{ KeV},$$

$$E_{I\varepsilon} = E_b \cdot \sin^2\theta \cdot \cos^2\theta \cdot F(T_\varepsilon)$$

$$= (1 \text{ MeV}) \cdot \left(\frac{1}{\sqrt{2}}\right)^2 \cdot (0.48) = 120 \text{ KeV}$$

$$E_{Iy} = E_b (1-f)^2 \cdot \sin^2\theta \cdot F(T_f)$$

$$= (1 \text{ MeV}) \cdot (1-0.9)^2 \left(\frac{1}{\sqrt{2}}\right)^2 (0.3) = 1.5 \text{ KeV}$$

It is worth noting that while the relative impact energies E_{I0} (for zero-field) and $E_{I\varepsilon}$ (for optimum field) are comparable, E_{Iy} (for y-component-only field with f = 0.9) is two orders of magnitudes smaller. This significant quantitative difference between E_{Iy} and both E_{I0} and $E_{I\varepsilon}$ is brought about by the strength parameter f, and we will discuss the various consequences resulting from the differences among the three impact energies E_{Iy}, E_{I0} and $E_{I\varepsilon}$.

VI. DISCUSSION AND CONCLUSION

We start with the confinement-time-dependent function F(T) as defined by Eq. (43),

$$F(T) = 2(\frac{1}{\omega T})2\ [1-\cos(\omega T)]\ -2(\frac{1}{\omega T})\sin(\omega T) + 1,$$

where the confinement time T is set equal to T_0, T_f or T_ε in accordance with the respective field model [In Report II, T was set equal to $T_\parallel$].

Writing $\psi = \omega T$, we get

$$F(\psi) = 2(\frac{1}{\psi})^2\ (1-\cos\psi)\ -2(\frac{1}{\psi})\sin\psi + 1, \qquad (43')$$

which is graphically represented by Figs. 7(a) and (b). Note that $F(\psi)$ is an oscillating function with decreasing amplitude and approaches unity as $\psi \to \infty$. It has a maximum value of 1.6 at $\psi = 4.2$, and approaches zero as $\psi = 0$.

In terms of the confinement time T, we have $F(T) \to 1$ as $T \to \infty$. Since we have assumed a value of 5×10^{-5} Tesla for the geomagnetic field throughout our work, we get $\omega = 8.78\times10^{6}$ rad/sec. Thus, F is maximum at $T = 4.78\times10^{-7}$ sec. For $\psi = 0.0878$ or $T = 10^{-8}$ sec, we have the following approximate version of Eq. (43'):

$$F(T) \approx \frac{1}{4}(\omega T)^2 \qquad (43'')$$

Rewriting Eqs. (44) and (45) of Report II, together with Eqs. (44), (45) and (46), we have

$$E'_{IO} = E_b \sin^2\theta \cdot F(T_\parallel) \qquad (44')$$

$$E_{IO} = E_b \sin^2\theta \cdot F(T_o) \qquad (44)$$

$$E_I = E_b \sin^2\theta \cdot \cos^2\theta \; F(T_\parallel) \qquad (45')$$

$$E_{I\varepsilon} = E_b \sin^2\theta \cdot \cos^2\theta \; F(T_\varepsilon) \qquad (45)$$

$$E_{Iy} = E_b (1-f)2 \cdot \sin^2\theta \cdot F(T_f) \qquad (46)$$

For the zero-field and the optimum field models, we have used the corresponding "correct" confinement times T_o and T_ε instead ofthe approximate confinement time $T_\parallel$ as was done in Report II.

As shown by Fig. (6), T_o approaches a lowest value at $\theta \approx 90^o$, and increases at decreasing θ and is infinite at $\theta = 0^o$ while $T_\parallel$ has a minimum at $\theta = 45^o$, is symmetric with respect to $\theta = 45^o$, and diverges at $\theta = 0^o$ (90^o). Figs 5(a) to 5(h) show that T_ε diverges at both ends, is approximately linear with slightly lower value at lower range of θ, and can be regarded as qualitatively similar to $T_\parallel$.

The interesting <u>new</u> result obtains from the y-component-only field model as represented by Eq. (46) and is discussed below.

First of all, it should be noted that all the confinement times, $T_\perp$, T_o, T_ε and T_f are not rigorously valid at $\theta \approx 90^o$, because re-entry of electron into the beam path is not taken into account. Therefore, if we exclude large θ, all the T's are qualitatively similar, even though we have T_f (with $f > 0.9$) $> T_\varepsilon > T_o > T_\parallel$. It is worth mentioning that all the T's decrease very slowly with energy above 5 Mev.

Because of factor $(1-f)^2$ in Eq. (46), E_{Iy} is at least two orders of magnitude smaller than the other confinement times if f is assumed to be > 0.9. Therefore, E_{Iy} results in a comparatively larger ionization cross section, as

indicated by the energy versus cross section curve [See Fig. 8 of Report II.] Especially at small θ ($\theta < 10^{o}$), we have larger T_f, and also larger σ because of factor $\sin^2\theta$ in E_{Iy}.

Regarding T_f and σ (respectively, the collision time and collision cross section), we can offer a semi-quantative argument in favor of the y-component-only field model in terms of the relation

$$\tau = \frac{1}{\sigma n v} = \frac{1}{\sigma J}$$

where τ is the time between collisions, n is concentration per cm^3, v is the beam velocity, and $nv = J$ is the beam current density.

With $J = 1A/cm^2$, $\delta = 10^{-16}cm^2$, we have $\tau = 10^{-3}sec$, which is a rather long time. However, for $f > 0.95$, $\theta < 10°$, and especially with $E_b < 1$ MeV, we obtain a confinement time T_f comparable to τ.

Another physical consideration, also in favor of the y-component-only field model is the following. The time scale of beam operation is probably too short for the build-up of "optimum" space-change field as described in Report II; thus, a partial ($f < 1$) y-component-only field is a more likely possibility. In fact, y-component-only polarization field was suggested and observed [see Ref. 3 of Report II.]

In conclusion, we can say that our present work suggests that the partial y-component-only field model is a physically more reasonable, and thus, is a more likely physical mechanism involved in the self-stripping. Conversely, if the actual polarization field corresponds to the partial y-component-only field model, as studied here, we can expect the self-stripping process to be significantly enhanced.

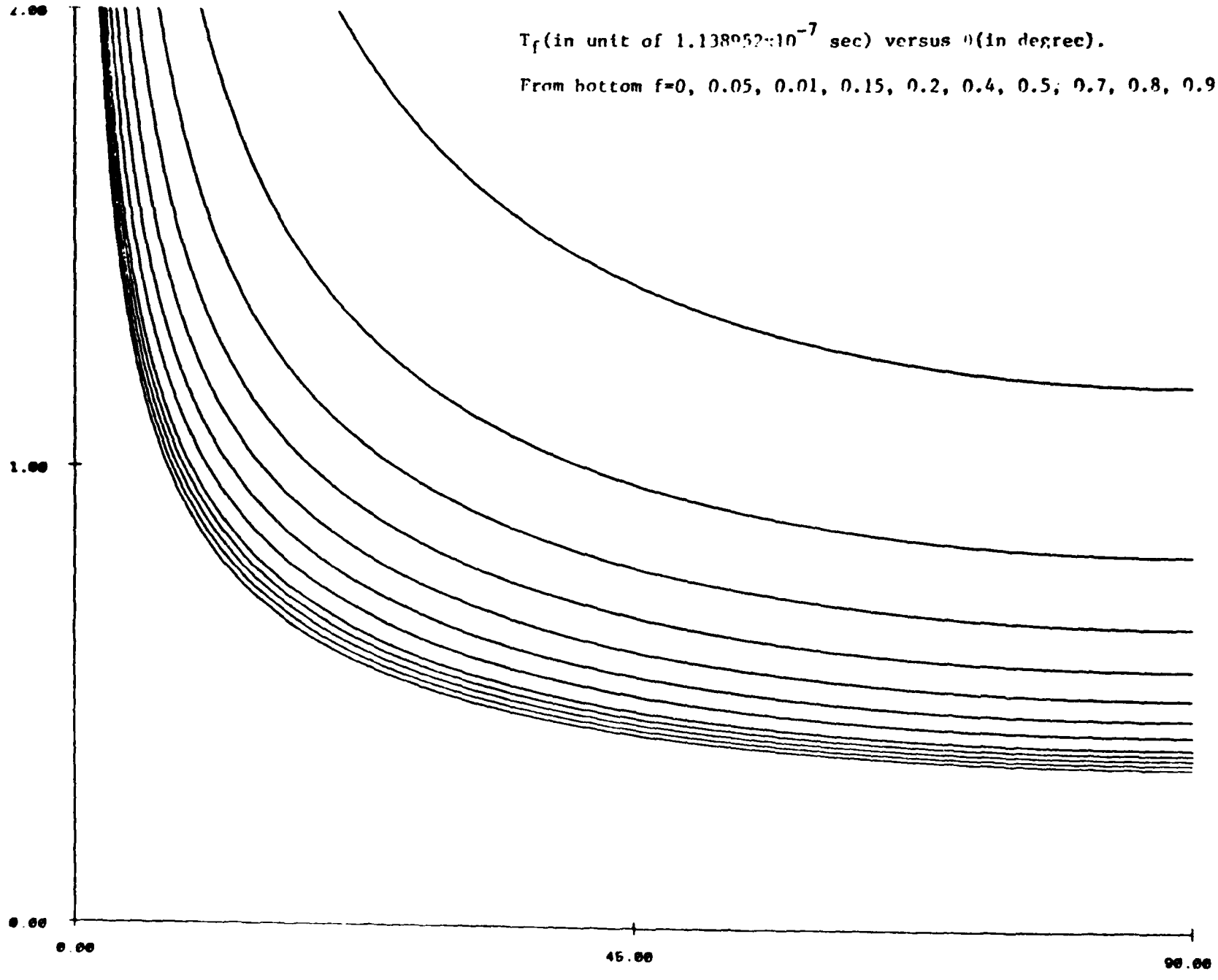
T_f(in unit of 1.138952×10^{-7} sec) versus θ(in degree).
From bottom f=0, 0.05, 0.01, 0.15, 0.2, 0.4, 0.5, 0.7, 0.8, 0.9 at tor
1.00
0.00
0.00
45.00
90.00

FIGURE 3(a) n=1

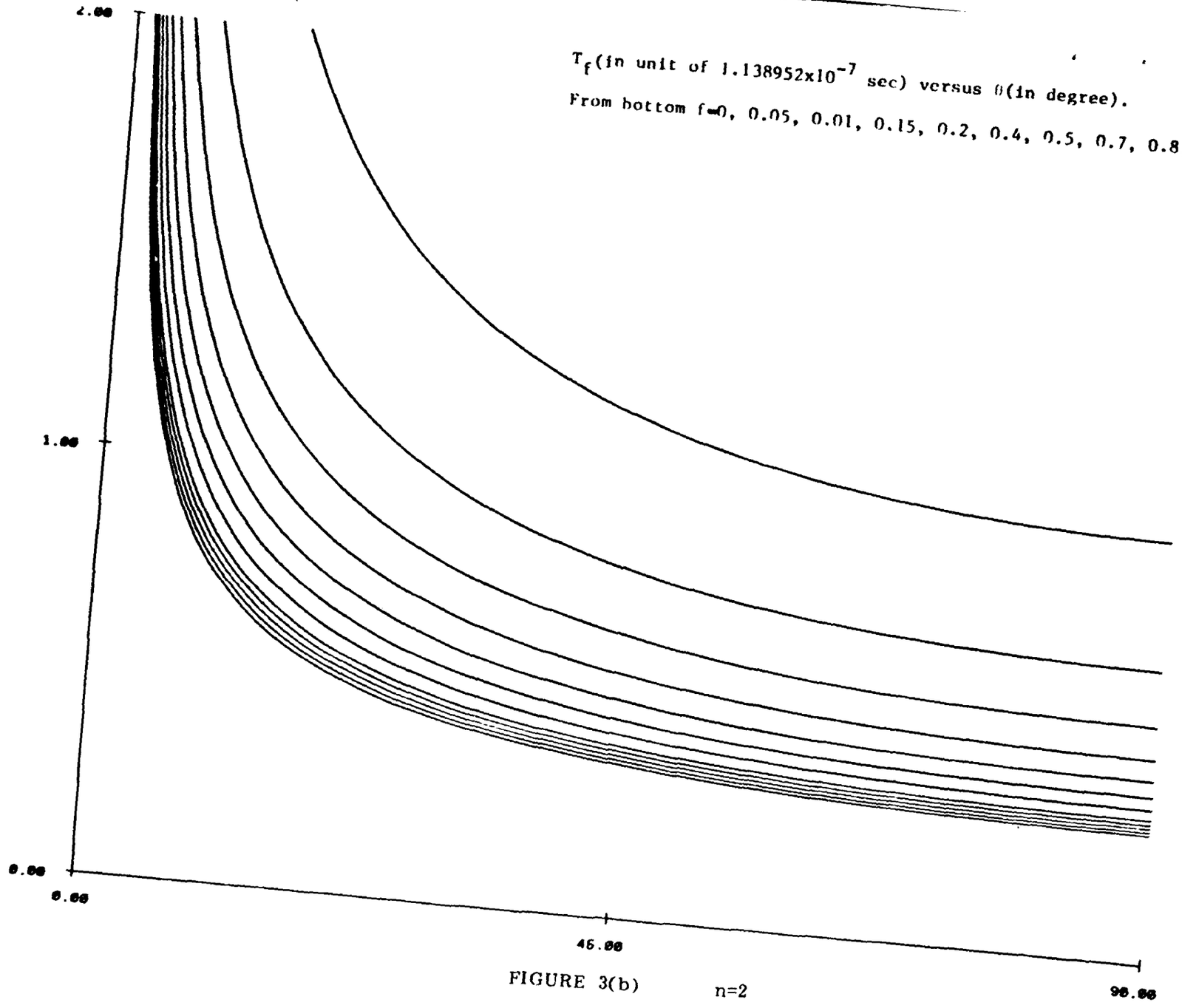
T_f(in unit of 1.138952×10^{-7} sec) versus θ(in degree).
From bottom f=0, 0.05, 0.01, 0.15, 0.2, 0.4, 0.5, 0.7, 0.8, 0.9 at top.
2.00
1.00
0.00
0.00
45.00
90.00

FIGURE 3(b) n=2

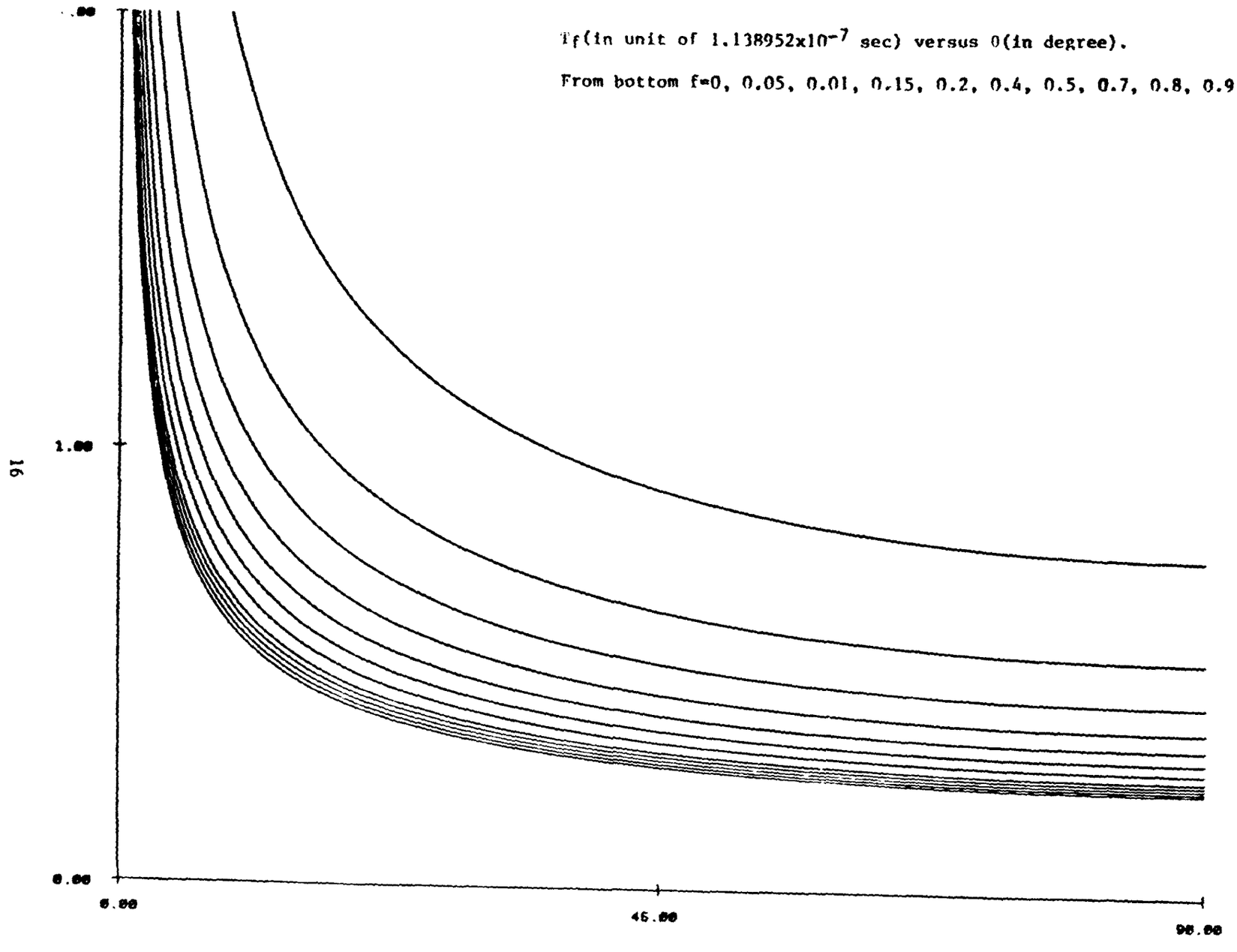
T_f(in unit of 1.138952×10^{-7} sec) versus θ(in degree).
From bottom f=0, 0.05, 0.01, 0.15, 0.2, 0.4, 0.5, 0.7, 0.8, 0.9 at top
16
1.00
0.00
0.00
45.00
90.00

FIGURE 3(c) n=5

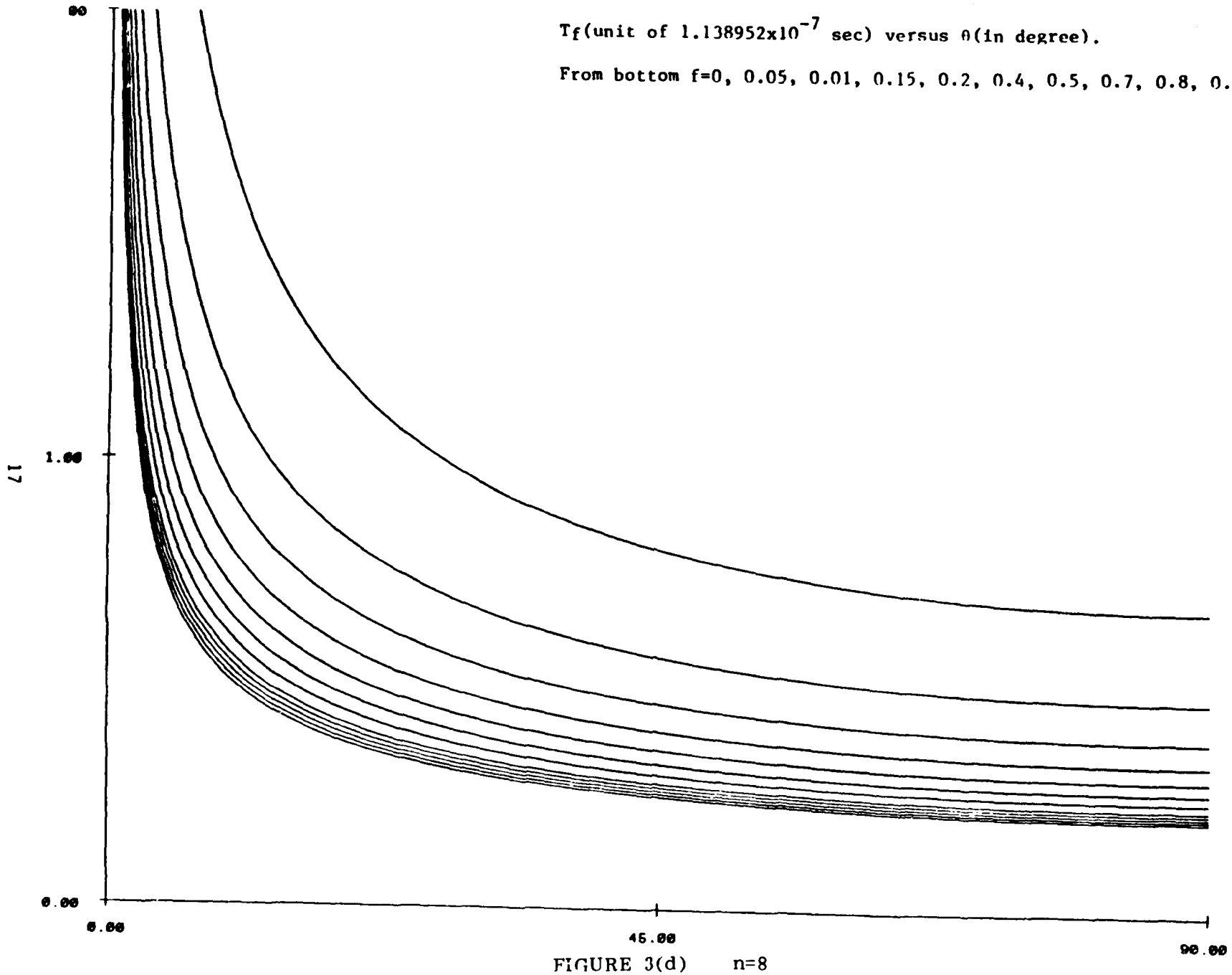
Tf(unit of 1.138952x10^-7 sec) versus θ(in degree).
From bottom f=0, 0.05, 0.01, 0.15, 0.2, 0.4, 0.5, 0.7, 0.8, 0.9 at top.
00
1.00
0.00
0.00
45.00
90.00

FIGURE 3(d) n=8

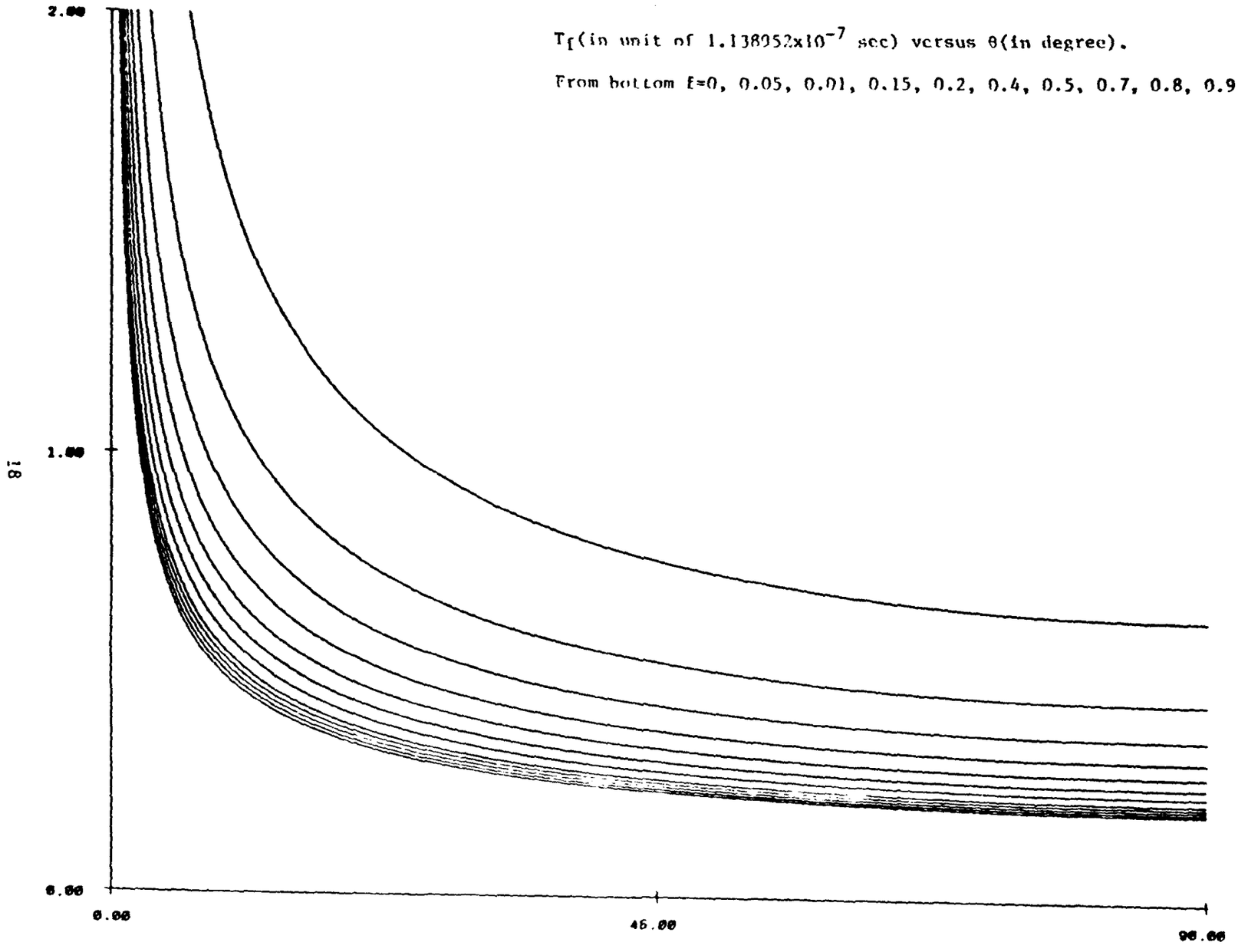

FIGURE 3(e) n=10

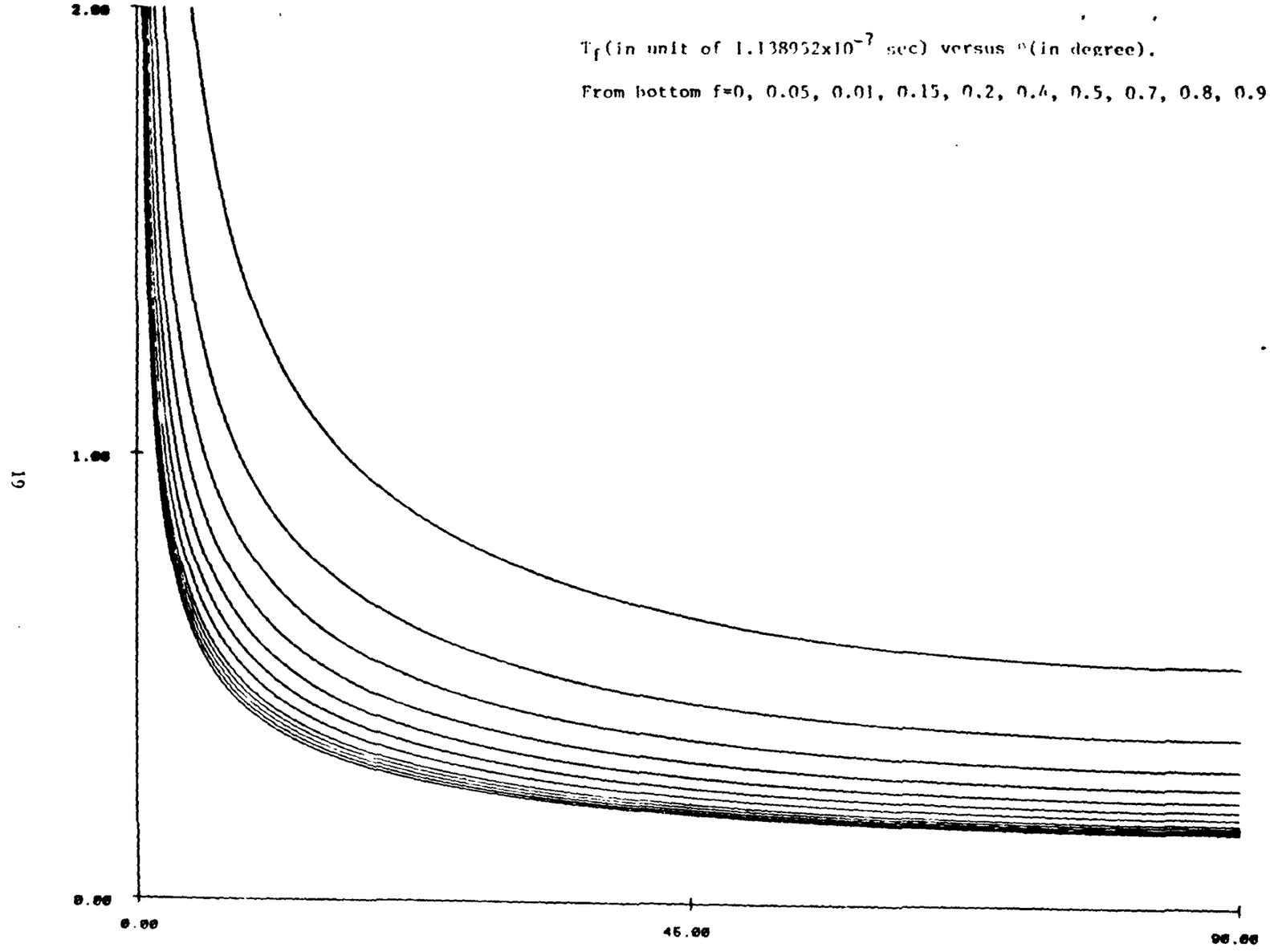

FIGURE 3(f) n=20

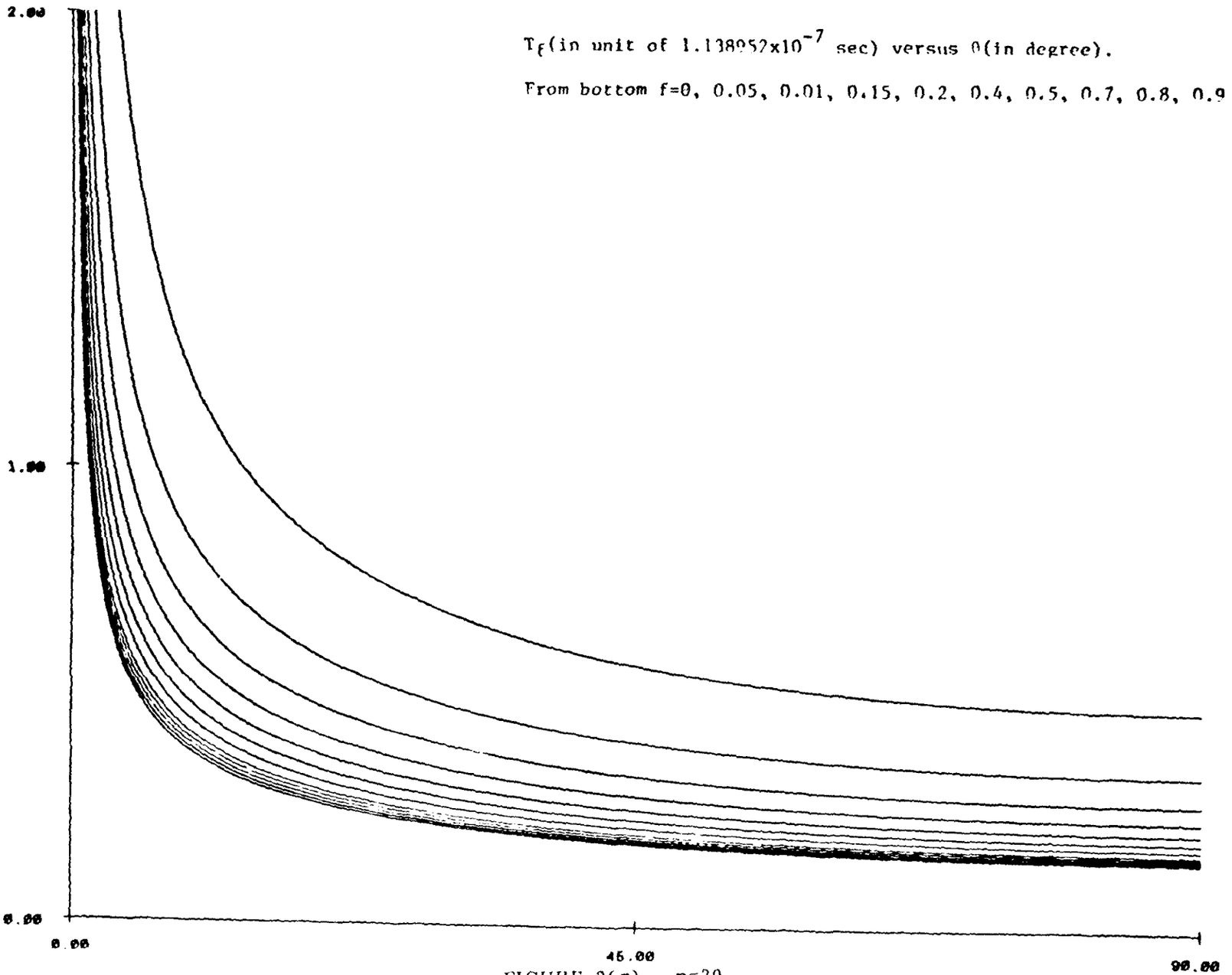

FIGURE 3(g) n=30

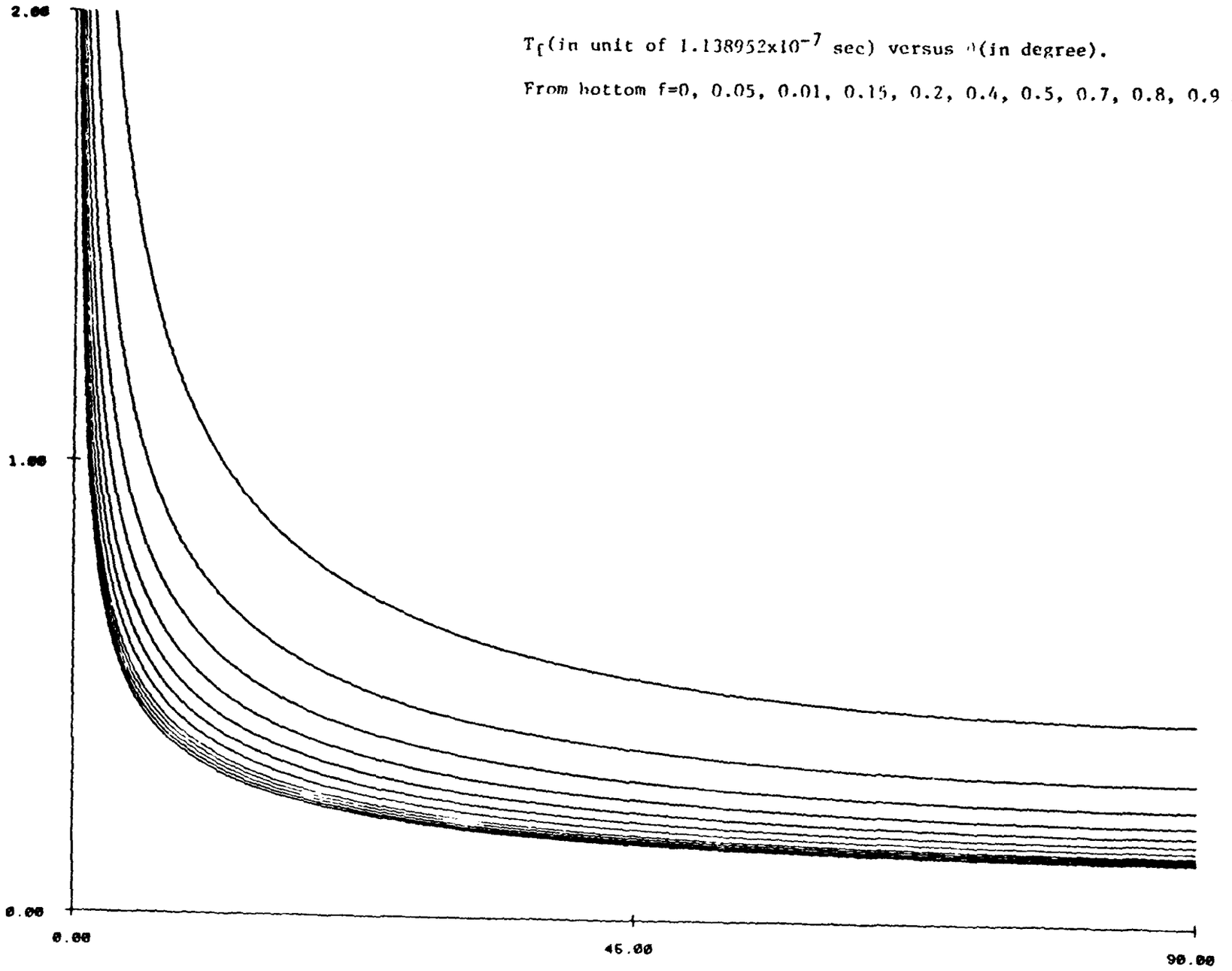

T_f(in unit of 1.138952×10^{-7} sec) versus θ(in degree).

From bottom f=0, 0.05, 0.01, 0.15, 0.2, 0.4, 0.5, 0.7, 0.8, 0.9 at top.

FIGURE 3(h) n=40

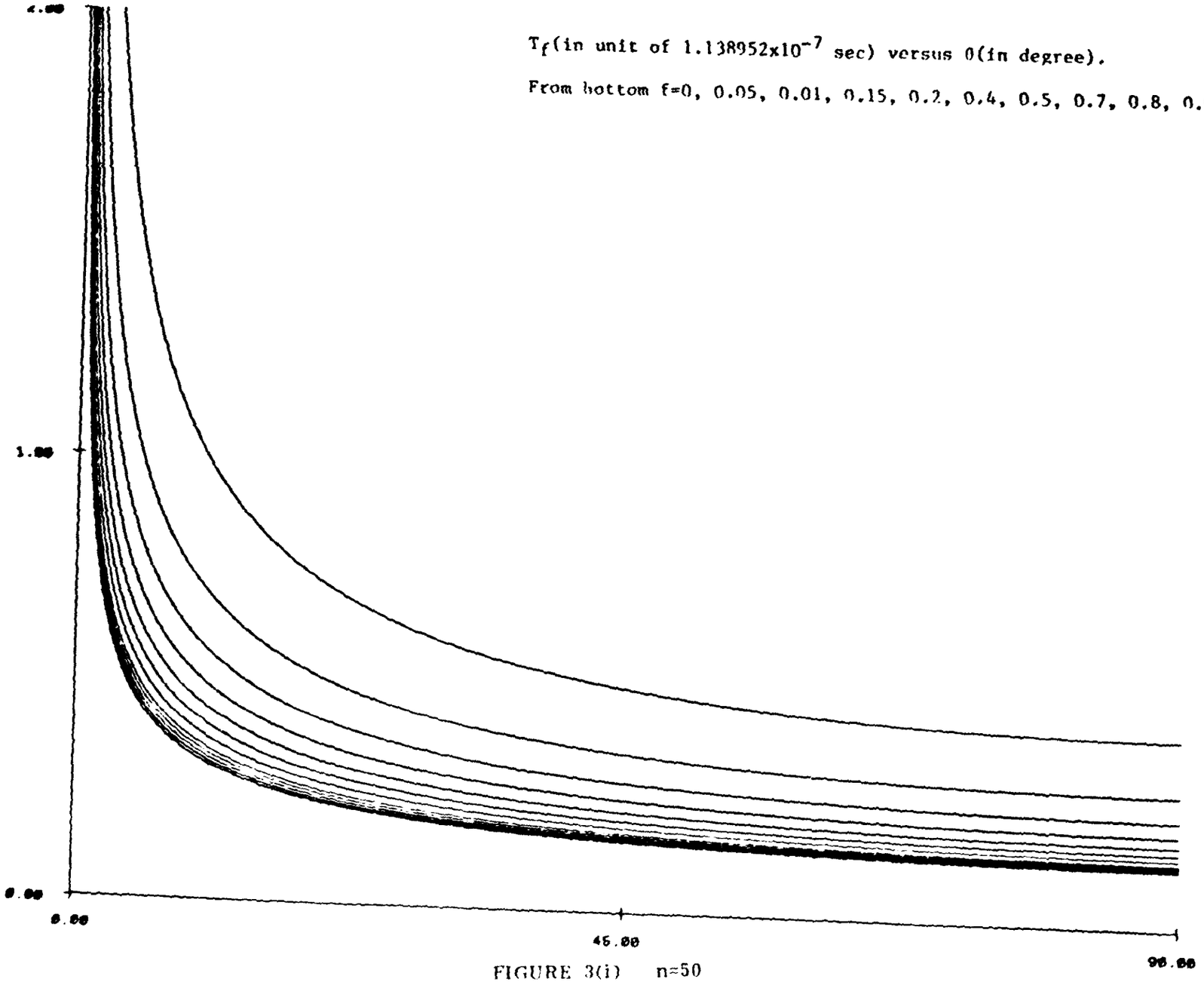

FIGURE 3(i) n=50

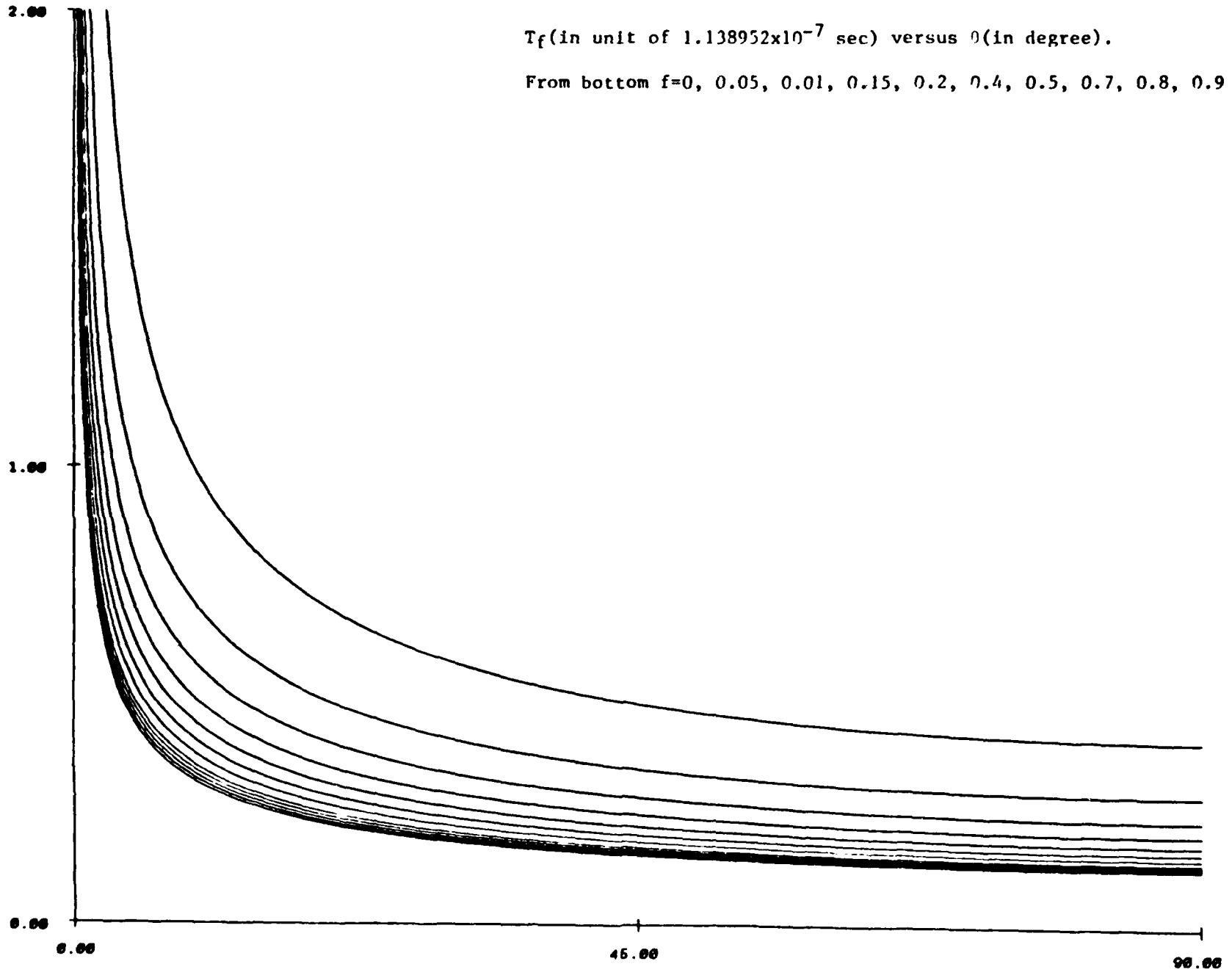

FIGURE 3(j) n=60

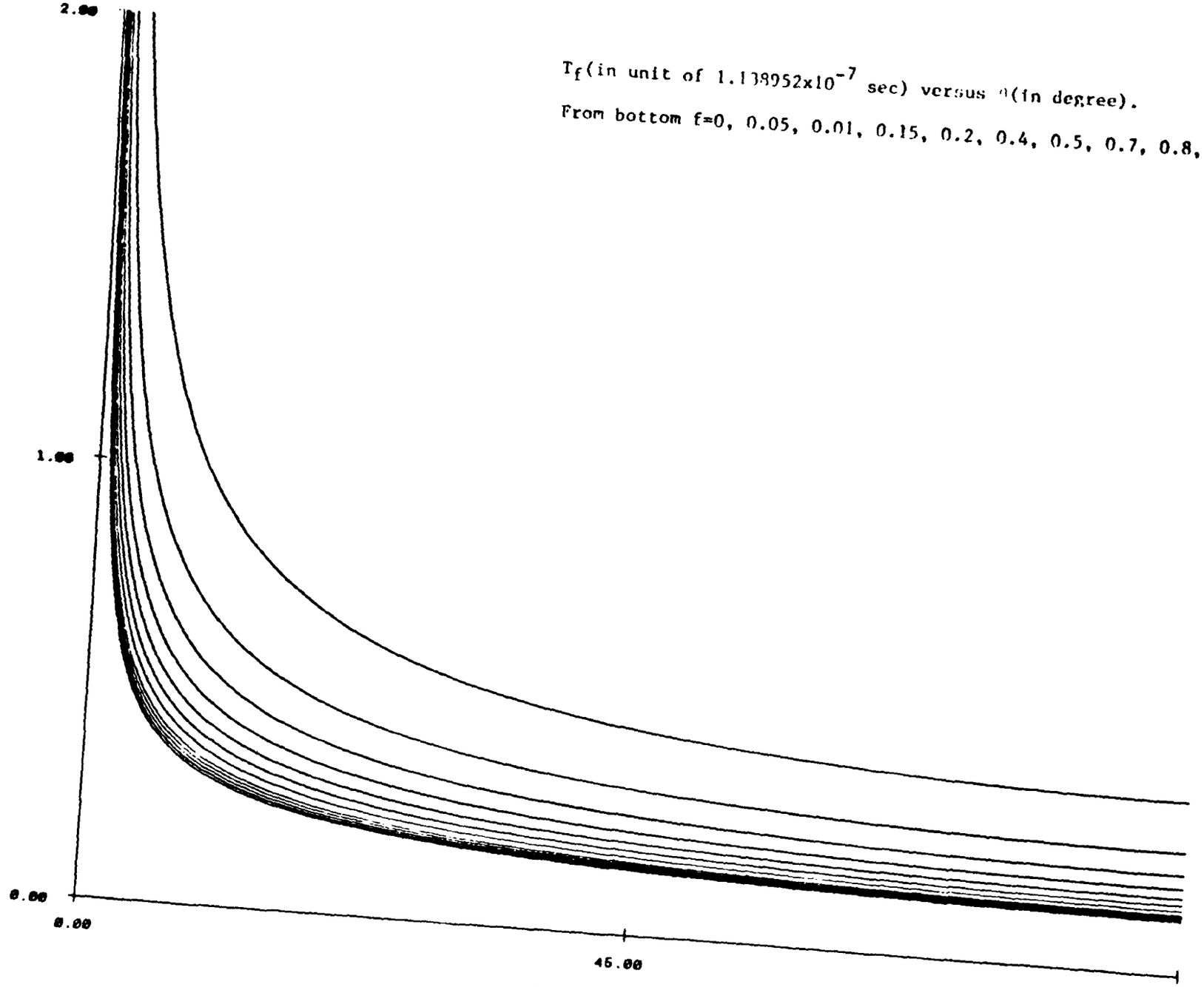

T_f(in unit of 1.138952×10^{-7} sec) versus θ(in degree).

From bottom f=0, 0.05, 0.01, 0.15, 0.2, 0.4, 0.5, 0.7, 0.8, 0.9 at top.

FIGURE 3(k) n=70

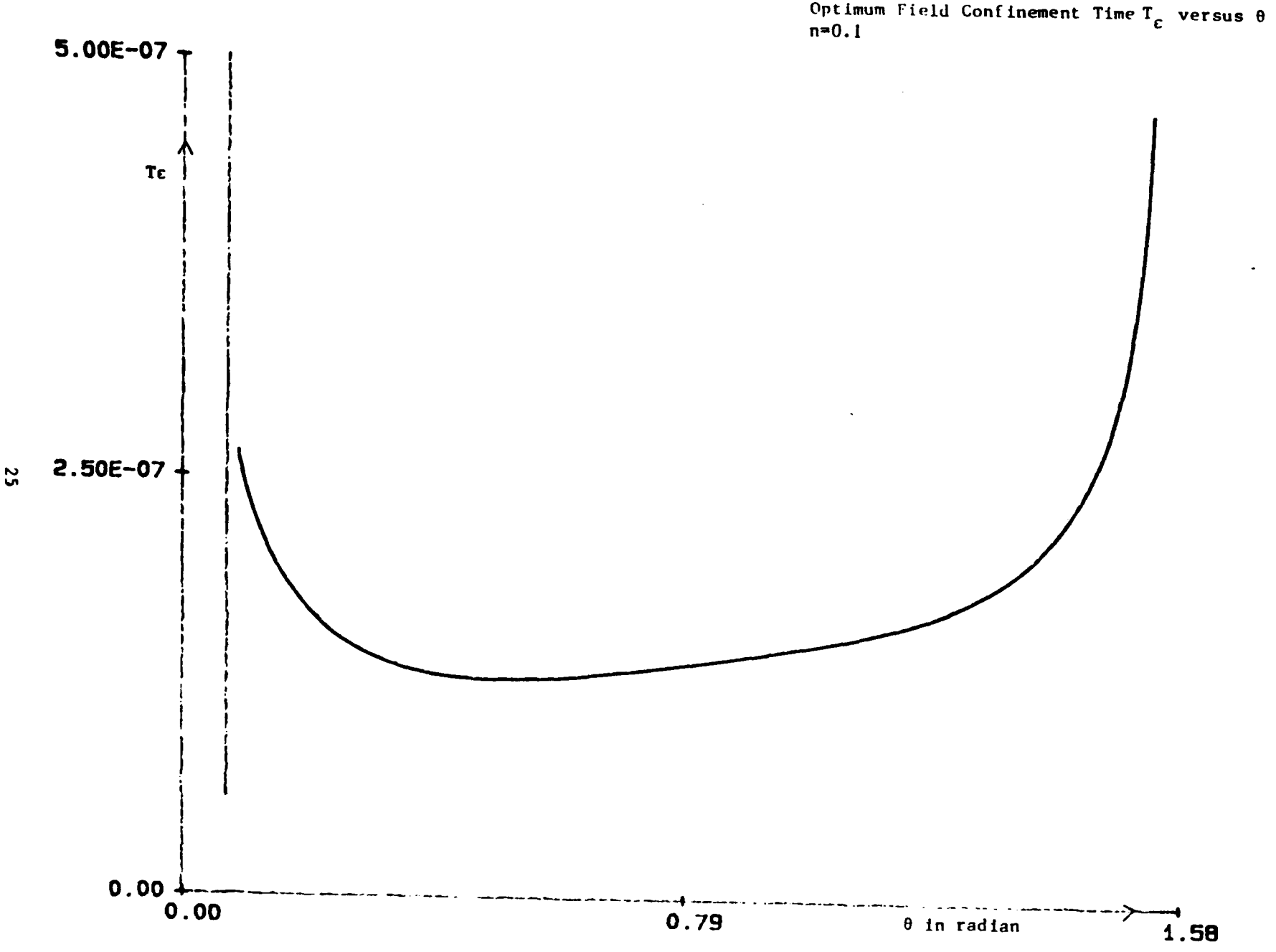
Optimum Field Confinement Time T_ε versus θ
n=0.1
5.00E-07
Tε
2.50E-07
0.00
0.00
0.79
θ in radian
1.58

FIGURE 5(a)

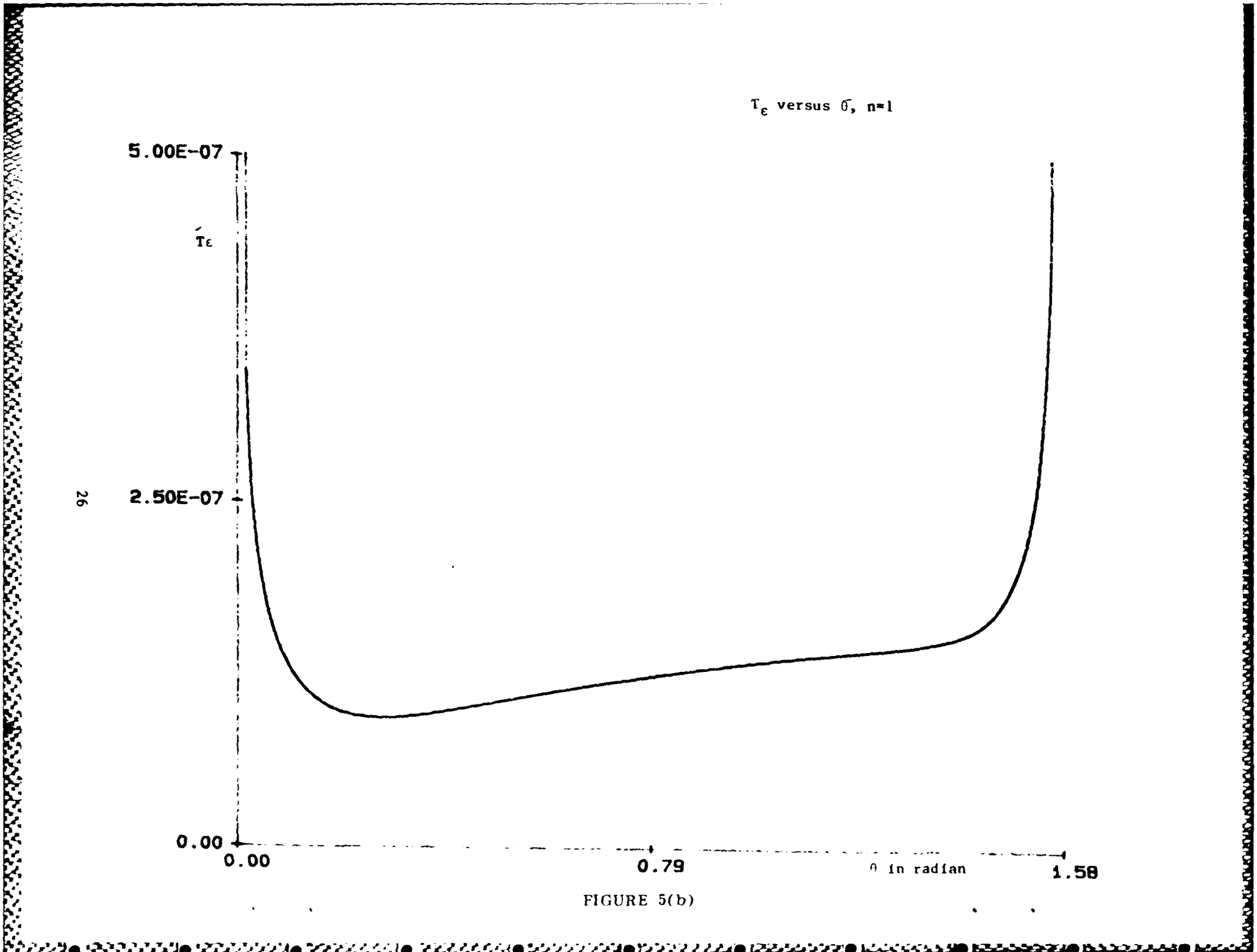
T_ε versus σ, n=1
5.00E-07
$\acute{T}\varepsilon$
2.50E-07
0.00
0.00
0.79
θ in radian
1.58

FIGURE 5(b)

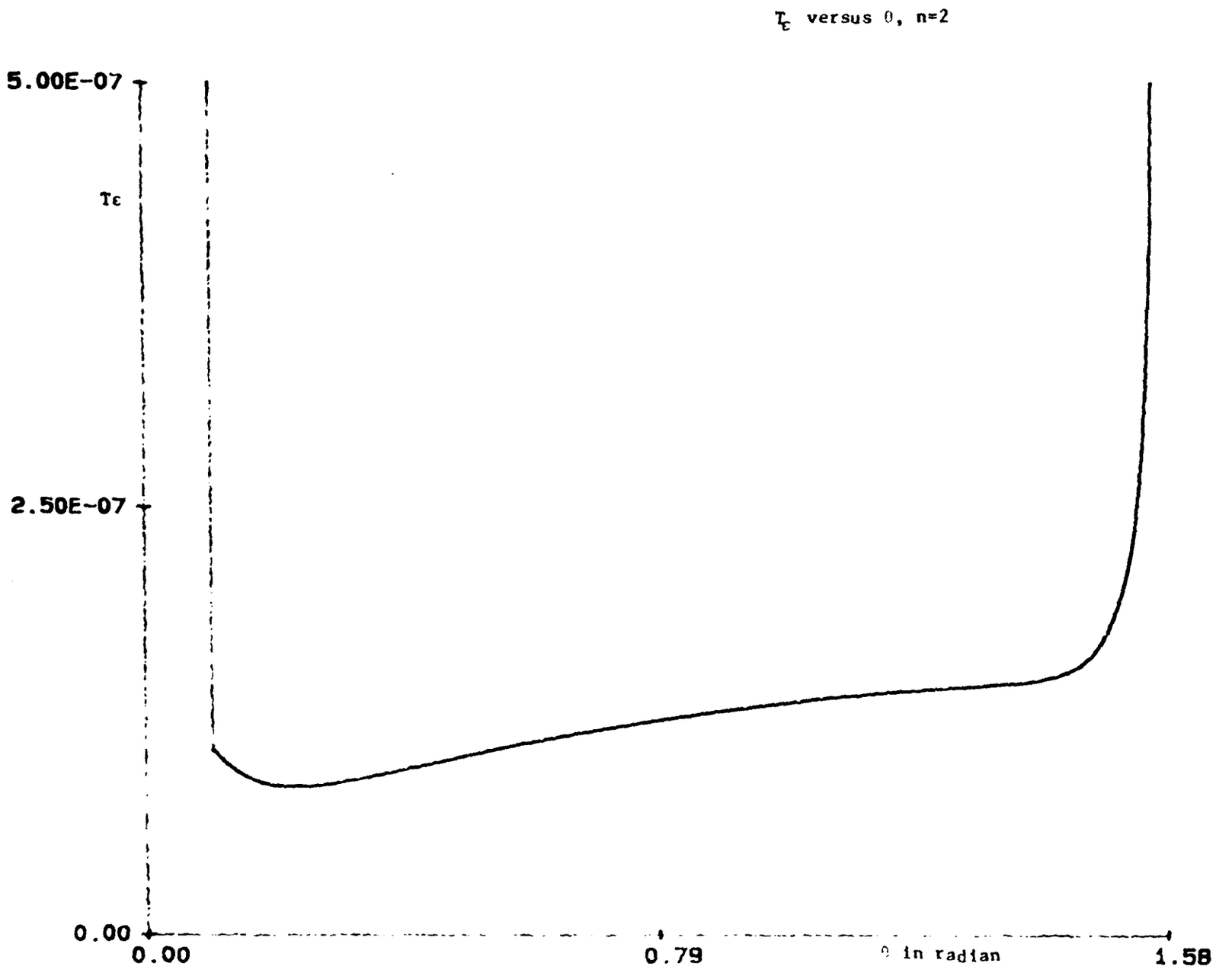
τ_ε versus 0, n=2
5.00E-07
τ_ε
2.50E-07
0.00
0.00
0.79
0 in radian
1.58

FIGURE 5(c)

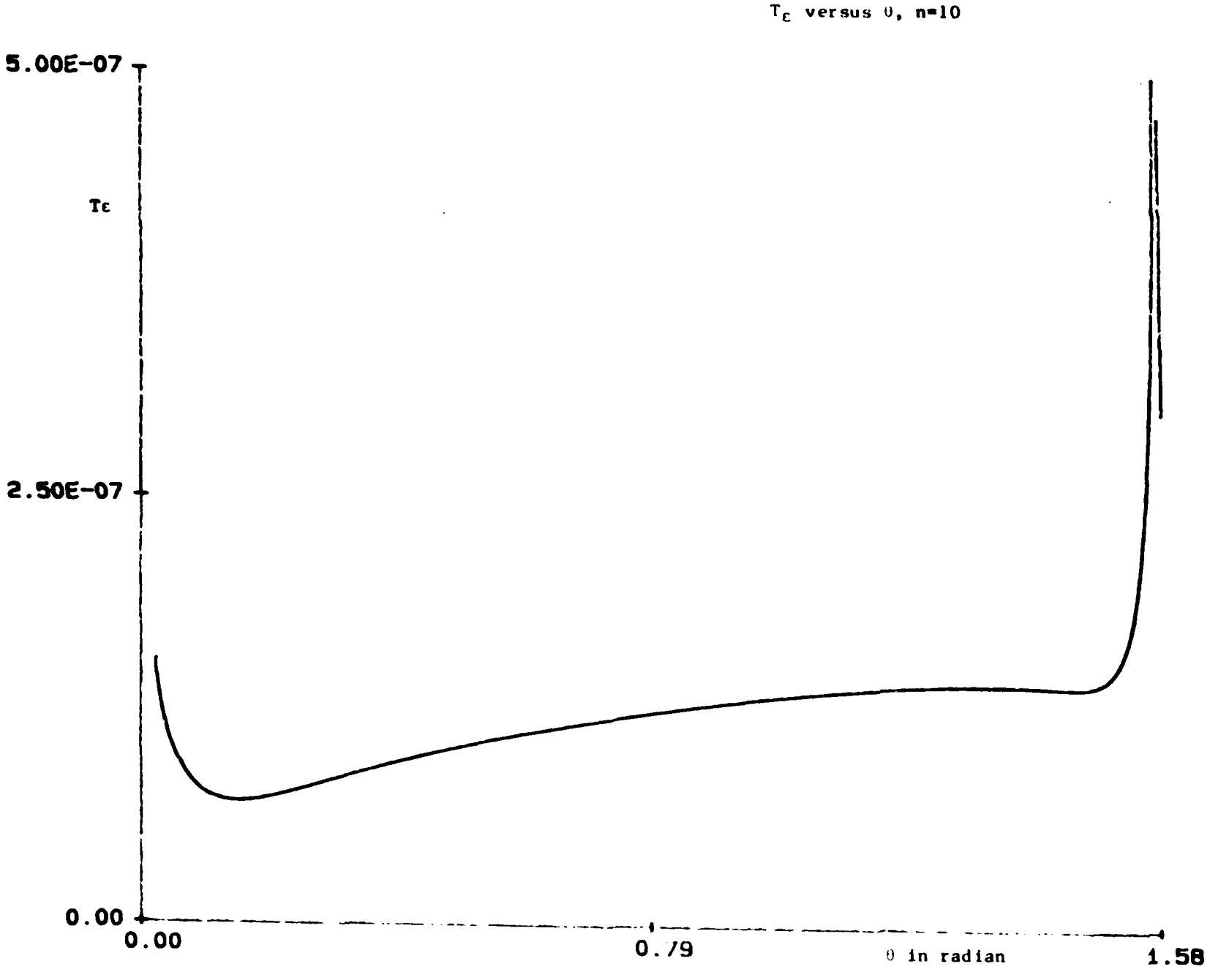
T_ε versus θ, n=10
5.00E-07
Tε
2.50E-07
0.00
0.00
0.79
θ in radian
1.58

FIGURE 5(d)

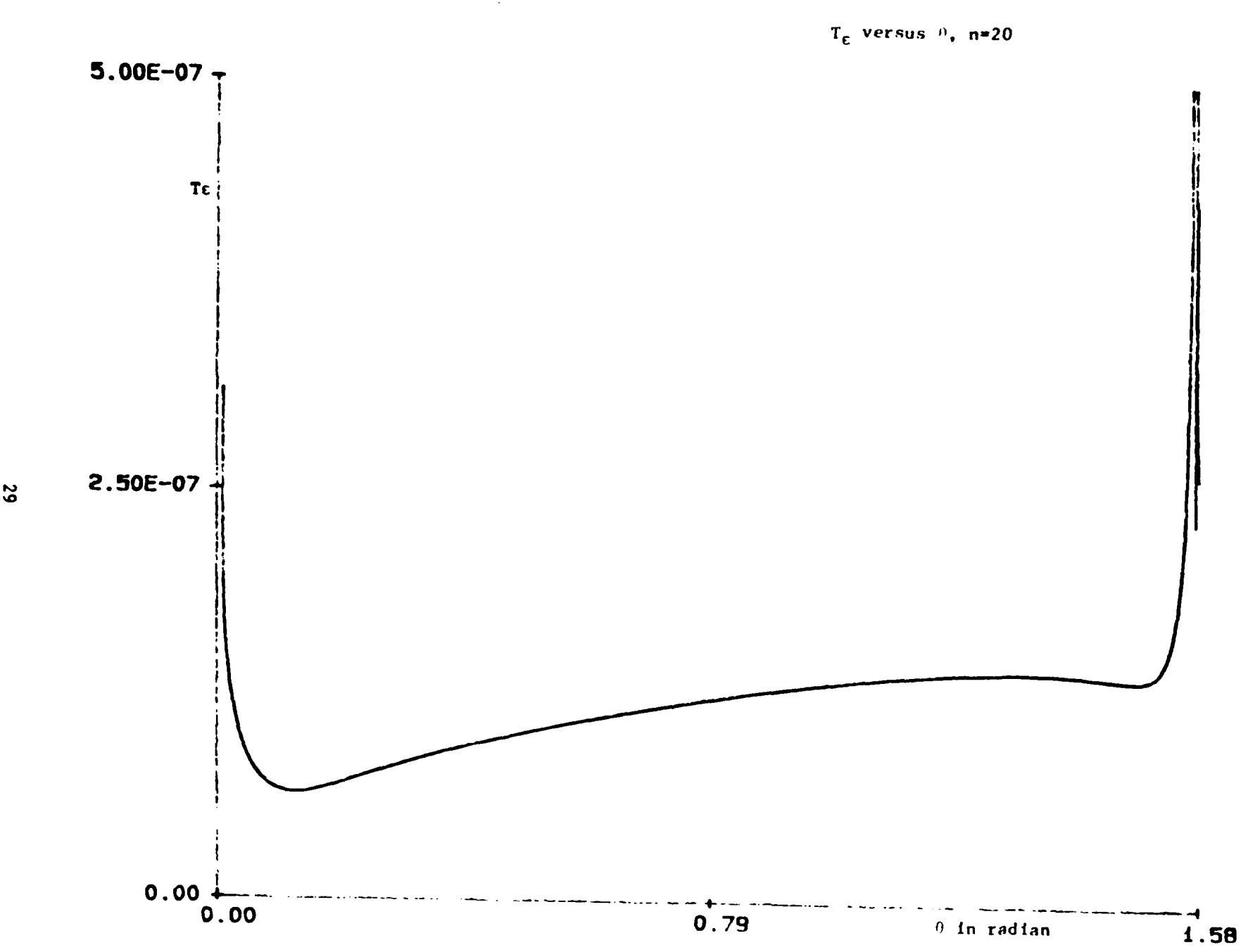
T_ε versus θ, n=20
5.00E-07
Tε
2.50E-07
0.00
0.00
0.79
θ in radian
1.58

FIGURE 5(e)

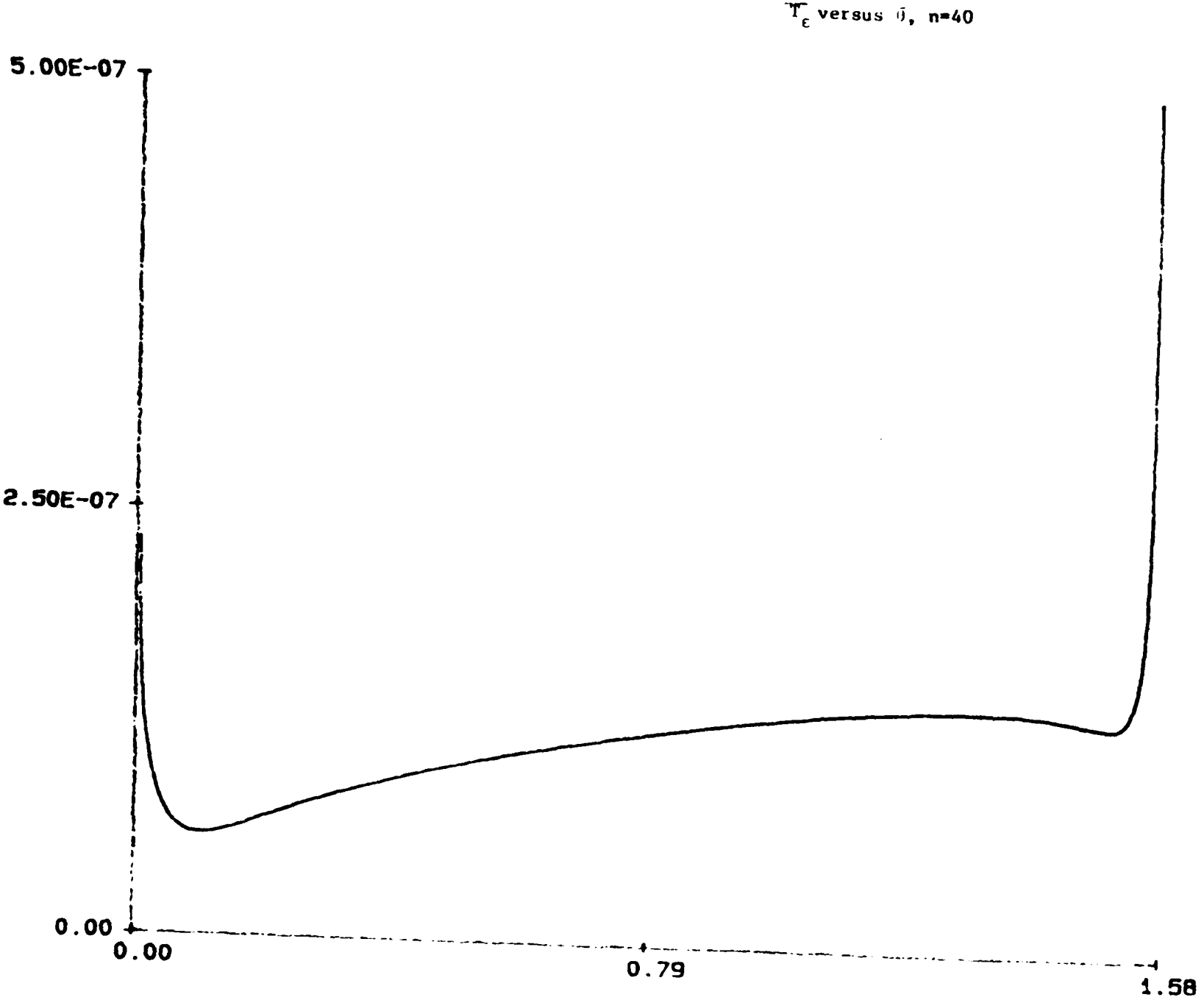
T_ε versus θ, n=40
5.00E-07
2.50E-07
0.00
0.00
0.79
1.58
ε_0

FIGURE 5(f)

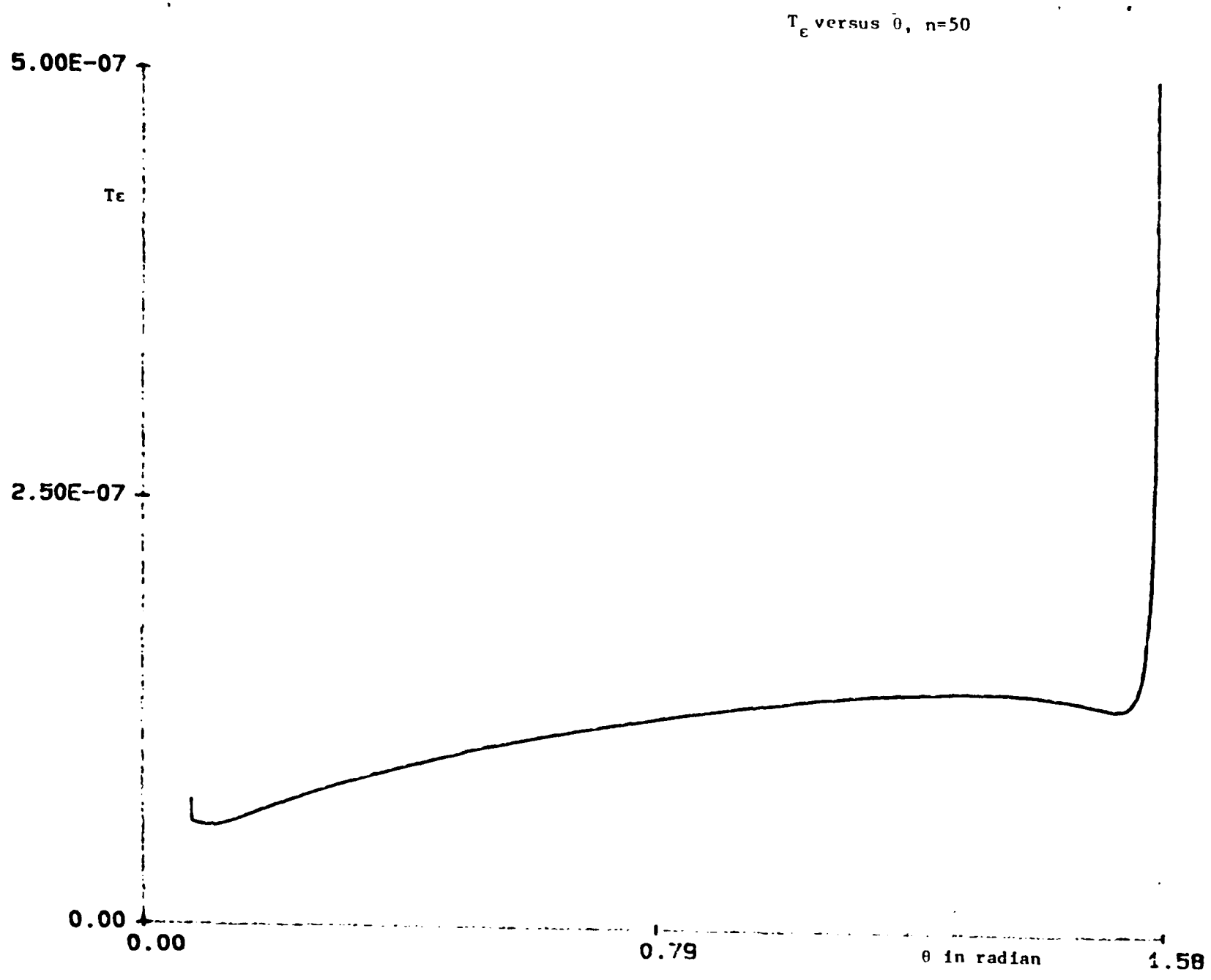
T_ε versus θ, n=50
5.00E-07
Tε
2.50E-07
0.00
0.00
0.79
θ in radian
1.58

FIGURE 5(g)

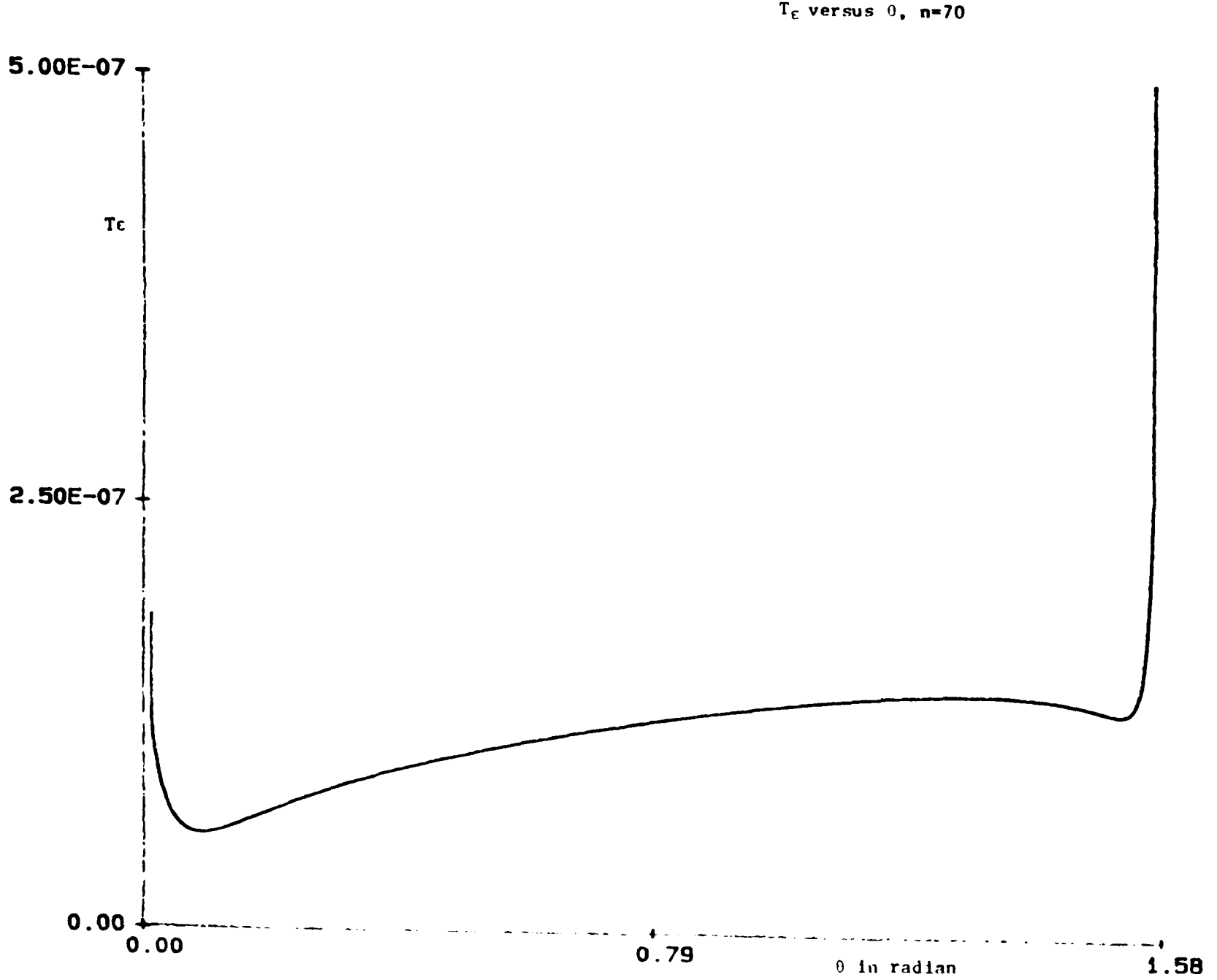
T_ϵ versus 0, n=70
5.00E-07
Tε
2.50E-07
0.00
0.00
0.79
1.58
0 in radian

FIGURE 5(b)

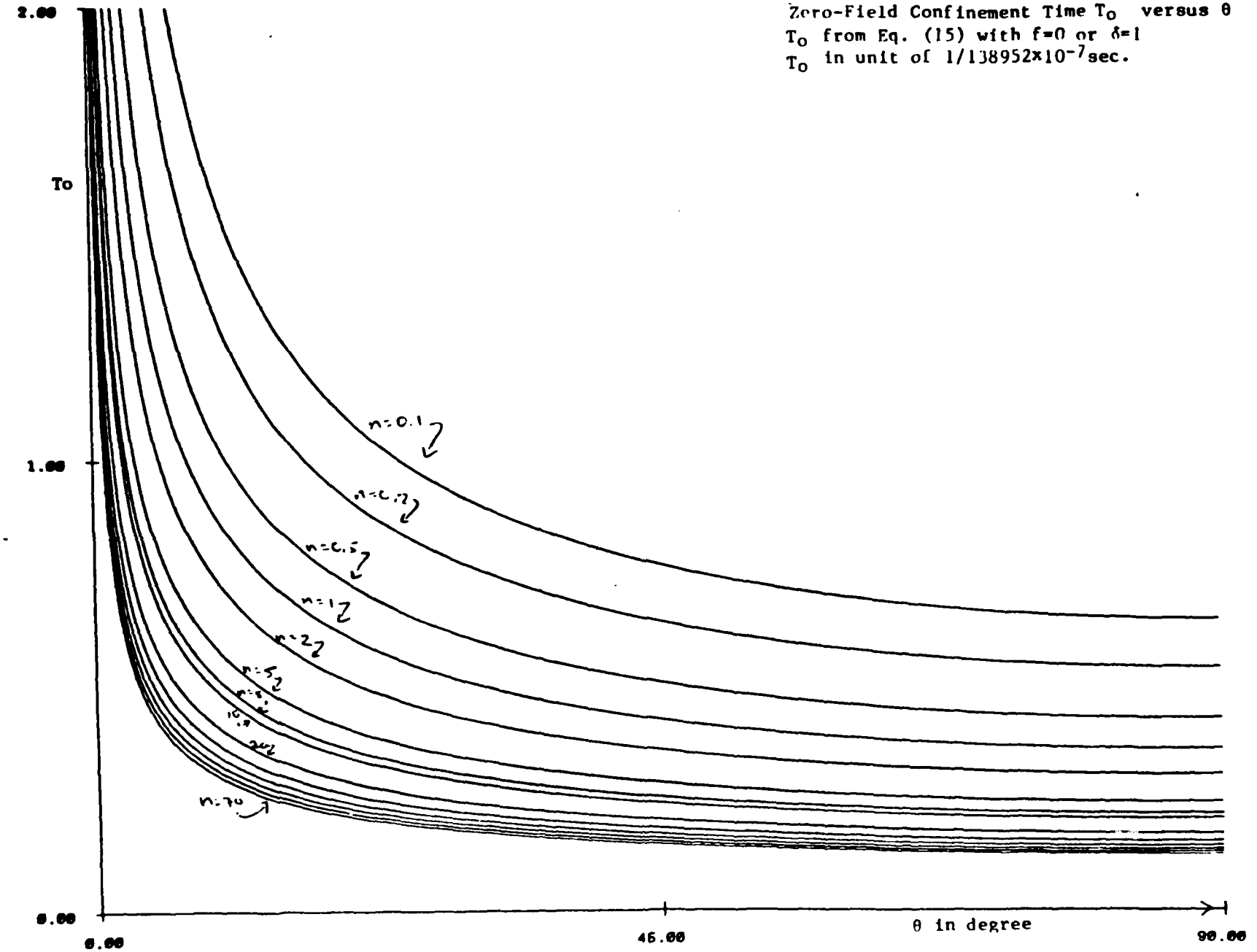
Zero-Field Confinement Time T_o versus θ
T_o from Eq. (15) with f=0 or δ=1
T_o in unit of $1/138952\times10^{-7}$sec.
2.00
To
1.00
0.00
n=0.1
n=0.2
n=0.5
n=1
n=2
n=5
n=10
n=20
n=70
0.00
45.00
θ in degree
90.00

FIGURE 6

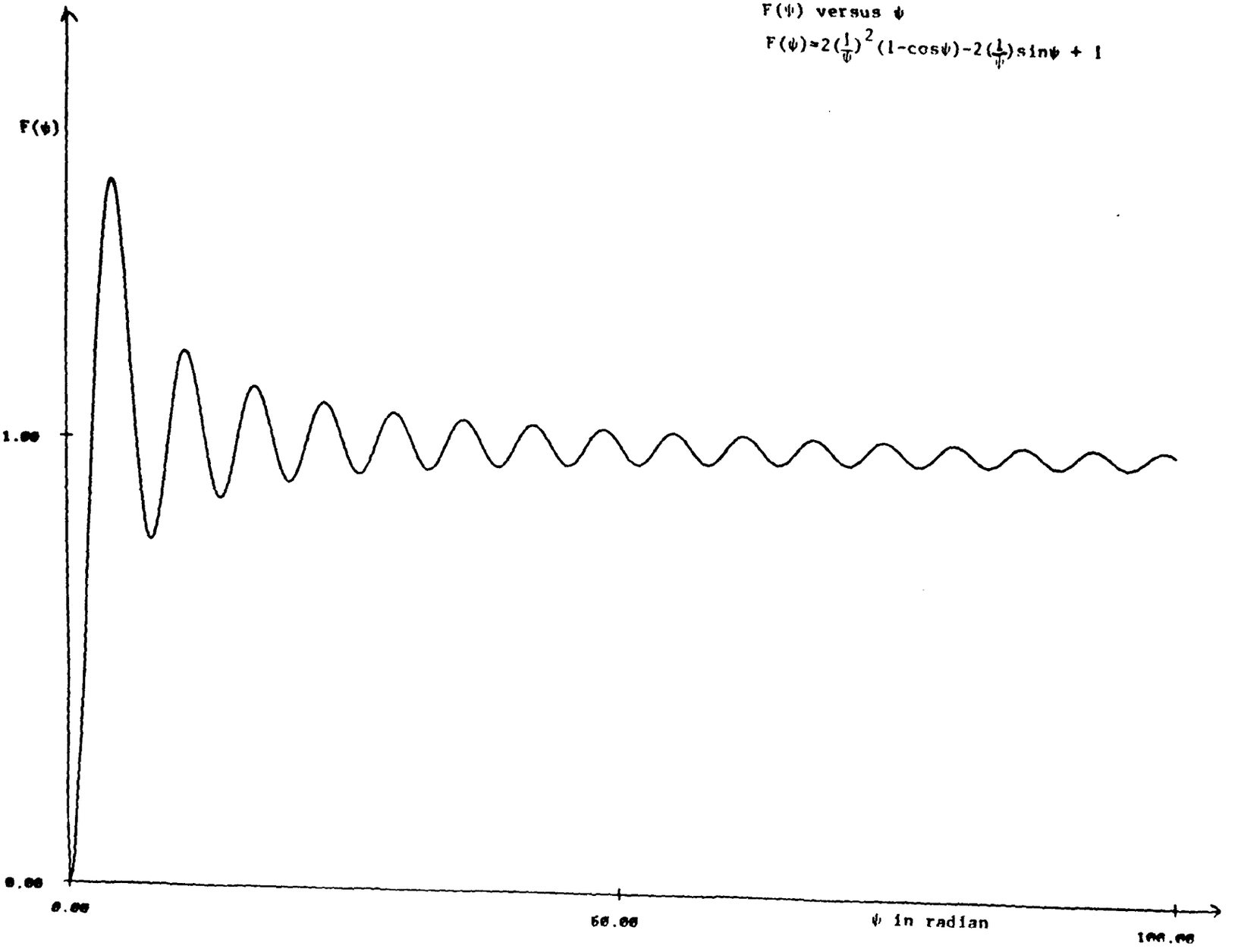
F(ψ) versus ψ
F(ψ)≈2(1/ψ)²(1-cosψ)-2(1/ψ)sinψ + 1
F(ψ)
1.00
0.00
0.00
50.00
ψ in radian
100.00

FIGURE 7(a)

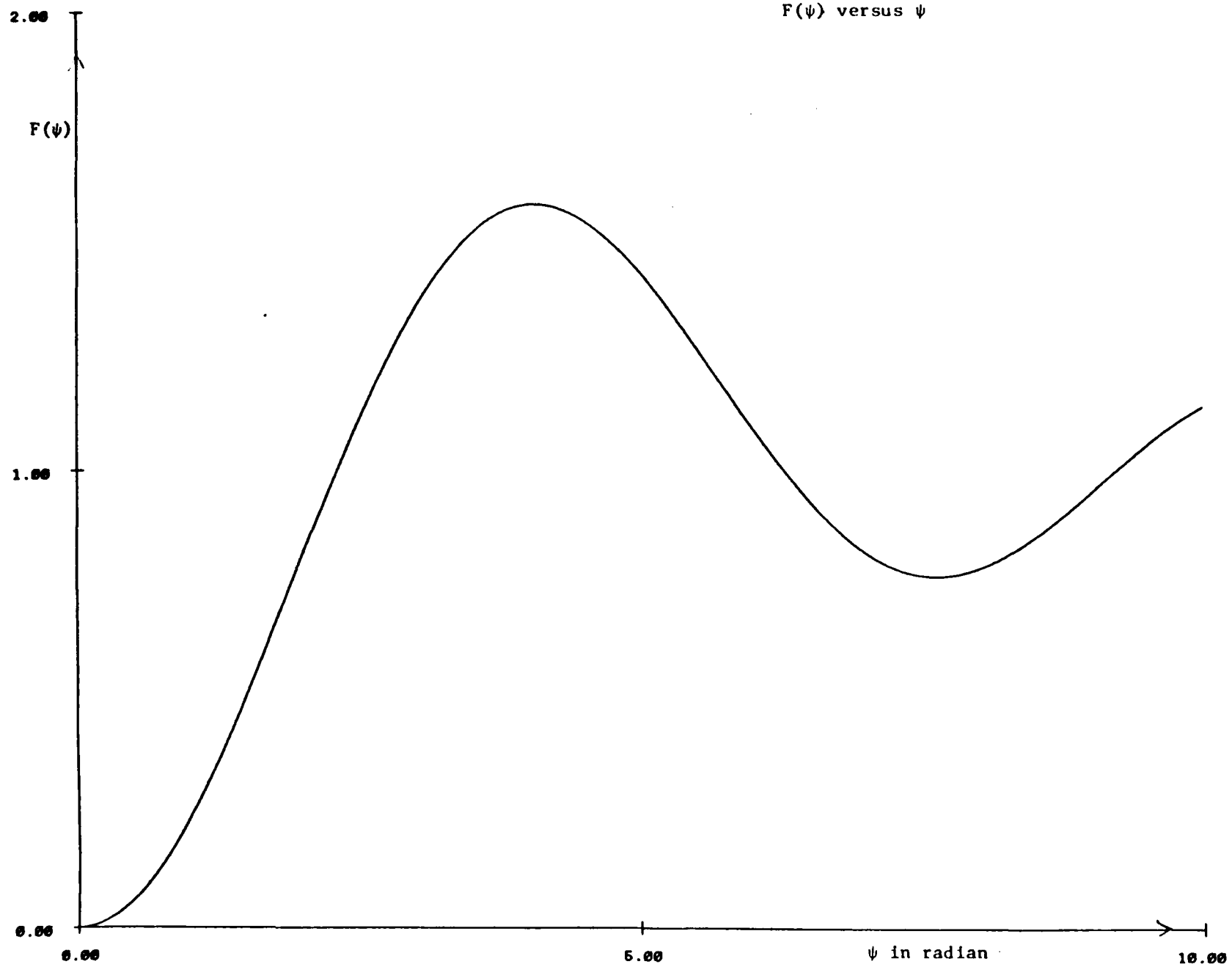

FIGURE 7(b)

END

DATE

FILMED

MARCH

1988

DTIC